The prediction of low- and mid-frequency internal road vehicle noise: a literature survey

N Lalor[1]* and **H-H Priebsch**[2]
[1]Institute of Sound and Vibration Research, University of Southampton, Southampton, UK
[2]ACC Akustikkompetenzzentrum, Gesellschaft für Akustikforschung mbH, Graz, Austria

The manuscript was received on 19 October 2005 and was accepted after revision for publication on 14 November 2006.

DOI: 10.1243/09544070JAUTO199

Abstract: Over the past 40 years the low- and mid-frequency internal noise of road vehicles has been of increasing interest to both manufacturers and customers, and there have been many papers written on the subject. It is particularly important that manufacturers are able to predict the noise at an early stage of a new design so that expensive mistakes can be avoided. This paper reviews the relevant literature published over this 40 year period and concludes that the finite element method (FEM), and/or the boundary element method (BEM) are currently the most accurate ways of predicting this noise. However, although the emphasis of this review is on the low- and mid-frequency structure-borne aspect of the noise, other prediction methods (which are normally considered to be only applicable at high frequencies) are also considered. In particular, the statistical energy analysis (SEA) is shown to be an increasingly useful tool for predicting structure-borne noise, as is the newly developed FEM/SEA hybrid method. Other essentially high-frequency techniques are also considered in this review because recent research indicates that it might be possible to apply these methods over a broader frequency range than was initially envisaged.

Keywords: automobile internal noise, FEM noise prediction, BEM noise prediction, SEA noise prediction, FEM/SEA hybrid method

1 INTRODUCTION

Over the past 35 years many researchers have attempted to predict the internal noise of road vehicles. Much of this work has been concentrated in the 50 to 200 Hz frequency range, mainly because noise levels are usually highest in this region. Right from the start it has been recognized that low internal noise is an important marketing feature, particularly with cars. Thus, predictive models have been set up in an attempt to first analyse the problem and then to investigate possible solutions. It is a well-established fact that this low- and mid-frequency noise is predominantly structure-borne, i.e. is produced by acoustic radiation from the vibrating cabin walls that are mechanically (rather than acoustically) excited. Therefore, this paper concentrates on the structure-borne aspect of the problem.

* *Corresponding author: Institute of Sound and Vibration Research, University of Southampton, Highfield, Southampton SO17 1BJ, UK. email: nl@isvr.soton.ac.uk*

2 NOISE CHARACTERISTICS

In 1972 Jha and Priede published a paper [**1**] that explained the basic mechanism of car interior noise due to the vibrating cabin walls. Although now over 30 years old, their results are still quite typical of the general characteristics of modern-day cars. Figure 1, which has been reproduced from their paper, shows internal noise spectra of one of the cars that they tested at different road speeds. The spectra rise to a maximum at around 20 Hz and then decay at an average rate of about 25 dB per decade to well over 1 kHz. Equivalent noise spectra for commercial vehicles are quite similar in general shape although the frequency at which the maximum level occurs will vary according to the size of the vehicle. Exciting forces at wheel rotation frequencies produce the noise peaks around 20 Hz which, together with a couple of harmonics, are superimposed on top of this general trend. Similar peaks occur over a broad frequency band around 100 Hz due mainly to low order harmonics of engine firing (four-cylinder,

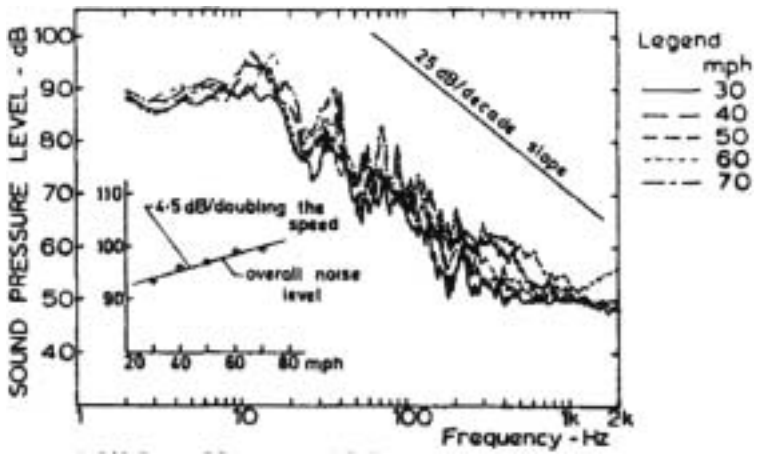

Fig. 1 Noise spectra inside car 'B' at various speeds

four-stroke engine) although, here, the spectrum shape is further complicated by the influence of low-order acoustic modes of the cabin space. These latter noise peaks, typically in the 50 to 200 Hz frequency range, are often referred to as low frequency 'boom'.

3 MECHANISMS OF INTERNAL NOISE GENERATION

Noise in the passenger cabin is the result of three different mechanisms:

1. *Direct transmission* from the outside through small holes in the cabin walls (e.g. at cable grommets) or through holes that are inadequately blocked acoustically (e.g. door seals). The 'slug' of air in the grommet hole or the floppy rubber seal in the door gap is set into vibration by the externally impinging acoustic wave, and it is mainly their mass that controls the amplitude of vibration. These then radiate noise directly into the cabin, although their small size means that this is generally only a problem at higher frequencies. For more details see, for example, reference [**2**].
2. *'Mass law' transmission* through cabin walls (e.g. from the engine compartment through to the bulkhead). The mechanism here is basically the same as in the previous case, i.e. it is the mass per unit area of the wall, not its resonant response, that is the dominating factor. However, since the radiating surface is now much larger it can generate noise at lower frequencies. For more details see, for example, reference [**3**].
3. *Acoustic radiation* into the cabin by the vibrating walls. The cabin walls are set into vibration either directly by external air turbulence or indirectly from engine and road inputs via the rest of the structure. In this case it is the resonant responses of the transmission paths and of the cabin walls that are the controlling factors. For more details see, for example, reference [**4**].

The above three mechanisms explain how vibrational energy enters the passenger cavity. Once it arrives there, the acoustic resonant response of the cavity also has a vitally important influence on the sound pressure experienced by the occupants. Figure 2, reproduced from reference [**1**], shows the internal sound pressure of a car due to an average roof acceleration level of 1*g*. The initial 25 dB per decade of decay is consistent with a reverberant acoustic field. The final flat portion indicates that free-field conditions now prevail but that the microphone is in the near field of the acoustic radiator. Between 50 and 200 Hz there is a transition zone where there is considerable scatter in the results. One of the difficulties in predicting 'boom' sound pressure levels is probably due to the fact that the basic mechanism of sound radiation is changing over this frequency range.

4 EXCITING FORCES

The three main sources of acoustic energy are the engine and its accessories, tyre/road interaction, and airflow over the vehicle body ('wind noise'). Although it is not strictly within the scope of this literature review to cover these sources, it is worthwhile at this stage to discuss them briefly.

The engine and its accessories as sources of noise and vibration have been studied for many decades and a large number of papers have been written on the topic. Reference [**5**] gives a comprehensive overview.

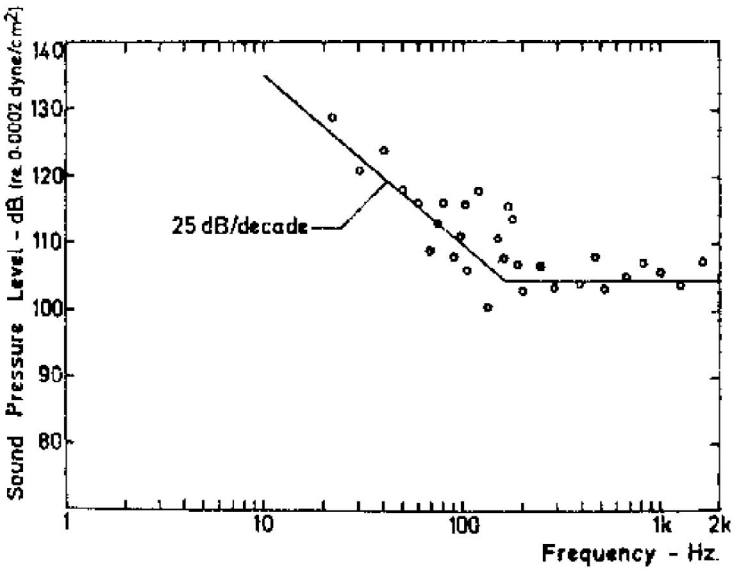

Fig. 2 Acoustic radiation inside car 'D' corresponding to an average roof vibration of 1*g*

Tyre/road noise has become increasingly important over the last few years as engine-related sources have been reduced to satisfy legislation requirements. There is a growing body of literature on the subject and, as examples, the reader is referred to papers by Kido *et al.* [**6**] (finite element modelling of tyres and suspension) and by Moeller and Pan [**7**] (statistical energy analysis (SEA) modelling of suspension and the rest of the car).

Figure 3, taken from reference [**8**], shows interior sound pressure spectra of a medium size family saloon car due to structure-borne and air-borne inputs from the above-mentioned sources. The results shown in the figure are for a vehicle speed of 100-km/h, which is too low for wind noise to be significant. It should be noted here that the structure-borne input to the rear was due solely to tyre/road interaction, whereas the structure-borne input to the front was due to a combination of tyre/road interaction and engine. It can be seen that below 500 Hz the interior noise is dominated by structure-borne inputs.

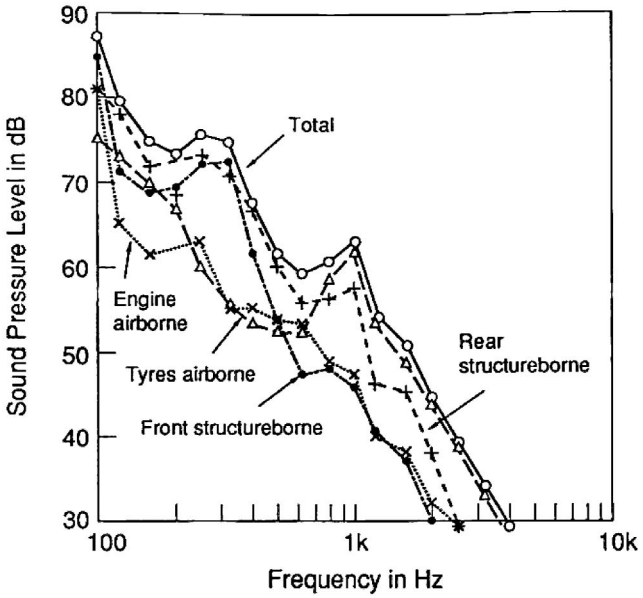

Fig. 3 Sources of interior noise

As well as tyre/road and engine noise, wind noise is also becoming increasingly important for similar reasons, although the problem is generally only significant at high speeds (wind noise increases at approximately 60 dB per decade of speed, which is a much higher rate than the other sources). In 1989 George [**9**] wrote a classic paper on the basic reasons why the airflow produces noise, although there are now many other papers on the subject. Strumolo [**10**] gives the mathematical background to the generation mechanisms and has produced a computer program, based on an SEA model, which claims to accurately predict the driver's ear sound pressure due to airflow once the CFD (computational fluid dynamics) calculation of external pressure has been carried out.

5 VARIABILITY OF INTERNAL NOISE

A very important consideration when predicting noise and/or vibration is variability. In 1984 Wood and Joachim [**11**] studied the variability of 12 nominally identical sedans. They found that variability was

d000000199 13-12-06 16:24:58 Rev 14.05
The Charlesworth Group, Wakefield 01924 204830

quite low up to about 50 Hz but, as frequency was increased to 200 Hz, 10 dB variations occurred. They studied the reasons for this and found that the variation in damping (mainly at the spot-welded and bolted joints) was the main culprit. The damping not only affects resonant amplitudes but also affects the phase. Thus, even if the amplitudes of the sound pressure contribution vectors from different panels (e.g. the windscreen) are constant, the vector sum can be significantly different.

More recently Kompella and Bernhard [**12**] tested 99 nominally identical Isuzu Rodeo saloon cars and 57 nominally identical Isuzu pickup trucks for variability. On each vehicle they measured a structure-to-acoustic transfer function (hammer impact on the left front wheel to the driver's ear SPL (sound pressure level)) and an acoustic-to-acoustic transfer function (under the floor loudspeaker to the driver's ear SPL). Their results are summarized in Table 1.

The fact that the variability below 500 Hz is significantly greater with the structure-borne tests than with the air-borne tests confirms that the structure is the main cause. Gårdhagen and Plunt [**13**] have analysed the statistics of vehicle noise variation in some detail and have also come to the conclusion that it is the damping, particularly at the joints, that is the main cause. The importance of this variation is, of course, that deterministic methods (e.g. as finite element method or FEM) are only able to predict the noise/vibration of one member of a population of nominally identical cars. Because joint damping cannot be accurately calculated, there is therefore no way of identifying that particular member beforehand. In spite of these difficulties many attempts have been made to overcome them and references [**14**] to [**16**] give uptodate analyses of the subject. These uncertainties in the actual damping value mean that errors of up to ± 5 dB are quite likely to occur. This would tend to suggest that either statistical prediction methods should be used or that deterministic methods (using averaged damping values) should be used to predict an average, rather than a particular, vehicle.

6 ANALYSIS OF SPECIFIC PREDICTION TECHNIQUES

In 1984 Sestieri *et al*. [**17**] considered that there were four main methods for sound transmission analysis, namely:

1. *Architectural (geometrical) acoustics*. This is essentially a 'ray tracing' technique. According to the authors, this technique is only appropriate when $\lambda \ll$ cavity dimensions; i.e. it only works at high frequencies. It is also not suitable for structure/acoustic coupling problems.
2. *Finite element and/or modal analysis*. This is mainly appropriate for low frequencies and low modal densities.
3. *Statistical energy analysis*. This is mainly appropriate for high frequencies and high modal densities.
4. *Integral formulation and/or non-local discretization methods*. This is basically related to the boundary element method (BEM) and, as such, is appropriate for coupled structure/acoustic problems.

More recently (1996) Wilby [**18**], in his review of aircraft noise, in addition to the above also lists closed-form solutions (mainly appropriate for aircraft cabins because of their regular shape) and power balance methods. This latter method, which consists basically of equating input acoustic power to the sum of the powers dissipated by damping in the side-wall trim and in the cabin, has some application to internal car noise prediction. This is because it is suitable for single frequency excitation at low frequencies, as shown by Rennison [**19**]. At high frequencies this technique is essentially the same as statistical energy analysis.

For the purposes of this literature review it was decided to modify Sestieri's classifications, mainly to take into account some modern developments. Accordingly, the classifications used in this paper are:

1. Finite element and boundary element methods
2. statistical energy analysis method

Table 1 Summary of FRF results (reprinted with permission from SAE paper 931272 © 1993 SAE International)

Description of measurements	Low frequency band	Variation (dB)	High frequency band	Variation (dB)
12 FRFs, reference, air-borne, RODEO	150–450	2	450–1000	4
12 FRFs, reference, structure-borne, RODEO	40–150	2	150–500	5
99 FRFs, air-borne, RODEO	150–450	4	450–1000	10
99 FRFs, structure-borne, RODEO	40–150	5	150–500	10
7 FRFs, reference, air-borne, truck	150–400	2	400–1000	4
7 FRFs, reference, structure-borne, truck	40–200	2	200–500	4
57 FRFs, air-borne, truck	150–400	5	400–1000	8
57 FRFs, structure-borne, truck	40–200	5	200–500	10

3. Hybrid methods
4. Ray tracing method
5. Band-averaged transfer function method

6.1 Finite element (FEM) and boundary element (BEM) methods

For the whole of the period covered by this literature survey, by far the most popular prediction techniques used by workers from all over the world are those based on deterministic models of the structural/acoustic system.

The initial attempts to predict cabin noise were focused on aircraft, mainly because of the very high noise levels entering the cabin from the engines and high-speed airflow. However, the relatively simple shape of the fuselage enabled existing closed-form analytical methods to be applied. An early (1983) example of such an application is given in a paper by Pope *et al.* [**20**], who demonstrated that good predictions could be obtained when compared with parallel model tests. A particular feature of their analysis is the modelling of the cabin sidewall acoustic lining. This is represented by a transfer matrix, which relates the sound pressure on the outside of the trim layer to that on the inside, the elements of this matrix being developed analytically. Later the same authors refined their model [**21**] and produced the PAIN (propeller aircraft interior noise) prediction program. Comparing predictions using PAIN with flight test results showed [**22**] that generally errors were less than 5 dB.

Apart from some relatively basic attempts to predict the noise inside cars (e.g. reference [**23**]), Koopmann and Pollard [**24**] were probably the first researchers to seriously apply the aircraft analytical solutions to cars. The authors assumed that the vibration of the body shell is unaffected by the acoustics (i.e. *in vacuo* conditions prevail) and that the enclosure is hard-walled as far as the acoustics are concerned. They argued that this is a realistic assumption because the generalized stiffness of the surrounding body structure is much greater than that of the enclosed air. They then defined a Green function, $G\omega$, which relates the acoustic pressure $p_\omega(r)$ at r, due to a source of volume velocity $v(r_0)\,\mathrm{d}A_0$ at r_0, as

$$p_\omega(r) = \mathrm{j}\omega\rho \int G_\omega(r/r_0)v(r_0)\,\mathrm{d}A_0$$

Because the cabin of a car is not of regular shape, this integral could not be explicitly evaluated. At the time the authors got over this problem by measuring G_ω experimentally, but it should be noted that this theory is essentially following the route taken by the later boundary element method (BEM). Another particularly interesting feature of this paper is the introduction of the concept of the joint acceptance function, J_ω, where

$$J_\omega = \frac{\int G_\omega(r/r_0)v(r_0)\,\mathrm{d}A_0}{\int |G_\omega(r/r_0)|\,\mathrm{d}A_0}$$

This function, which has the values $0 \leqslant J_\omega \leqslant 1.0$, defines how well a structural mode can drive an acoustic mode: 0 means no excitation whatsoever and 1.0 means the best possible excitation. The function is important because it is not necessarily the structural mode that is nearest in natural frequency to an acoustic mode that excites it most efficiently. Thus it is important to include enough modes when performing a forced response calculation by modal superposition. The authors claim that it is only necessary to include the two structural modes either side (in frequency) of an acoustic mode ('nearest neighbours'). However, since this conclusion was reached as a result of tests on a rectangular box which has uniform mode shapes and natural frequency sequences, it is probably wise to include rather more than this with an actual car.

By the early 1970s the finite element method (FEM) was a well-established technique for the analysis of structural problems. Because this method is now so widely used and understood, no description is given here. Readers not so familiar with the technique are referred to reference [**25**], which gives a very comprehensive description of the theory. In 1976 Petyt, Lea and Koopmann published [**26**] probably the first paper showing the formulation of a 20-node, isoparametric acoustic finite element. For verification purposes they built a one-twelfth scale model of a van cavity out of 10 mm thick perspex sheets (to ensure rigid boundary conditions) and measured the first 12 modes and natural frequencies. They then calculated these modes using a half finite element (FE) model (side-to-side symmetry assumed) consisting of eight elements. The computed mode shapes were in excellent agreement (although no MAC (media access control) number is quoted) and natural frequencies were within 2 per cent of the experimental values. It is quite surprising that over 5 years elapsed before other researchers took advantage of this highly significant development.

One of the first groups of researchers that did use finite elements to predict the internal noise of a vehicle (in 1982) was Nefske *et al.* [**27**]. They formulated the fully coupled problem by including a boundary surface acceleration vector in the equations of motion of the air and a boundary pressure vector in the equations of motion of the structure. They

stated that, ideally, these two sets of equations should then be solved simultaneously. However, due to the computer limitations of the time, they proposed that the problem could be considerably reduced in size by diagonalizing the matrices with a reduced modal matrix, the structural modes being computed assuming *in vacuo* conditions and the acoustic modes with a hard-wall assumption. Later (in 1985 and 1986) some of the same authors demonstrated this technique on a van [**28**, **29**], calculating the first 100 structural modes and first 20 acoustic modes using MSC/NASTRAN structural and acoustic finite elements. Figure 4, taken from reference [**28**], shows the authors' predicted and measured driver's ear sound pressure due to shaker excitation at the front bumper.

The fact that the computation has only been taken up to 100 Hz and that the errors start to become quite large above about 85 Hz. is not an inherent weakness of the technique but is probably because too few modes have been included. Agreement is generally within 5 dB at the peaks but the errors are much greater than this at the troughs. It should also be borne in mind that computation here is much simpler than with a car due to the more rectangular shape, the lack of trim, and the relatively hard seats.

Much discussion has taken place over the past 20 years concerning the necessity of having a fully coupled solution to the problem. The disadvantages of doing so are that it produces non-symmetric matrices and that the number of degrees of freedom are considerably increased (the solution now has to carry the combined structural and acoustic degrees of freedom). This can be seen from the coupled equations of motion, given in reference [**30**]

$$\begin{bmatrix} \mathbf{Maa} & 0 \\ \mathbf{Mca} & \mathbf{Mcc} \end{bmatrix} \begin{Bmatrix} \ddot{X} \\ \ddot{P} \end{Bmatrix} + \begin{bmatrix} \mathbf{Kaa} & \mathbf{Kac} \\ 0 & \mathbf{Kcc} \end{bmatrix} \begin{Bmatrix} X \\ P \end{Bmatrix} = \begin{Bmatrix} F \\ 0 \end{Bmatrix}$$

where

[**Maa**] = body mass matrix
[**Kaa**] = body stiffness matrix
[**Mcc**] = matrix of interior sound field mass
[**Kcc**] = matrix of interior sound field stiffness
{X} = body displacement vibration
{P} = sound pressure
{F} = exciting force applied to the body

Of course, the size problem can be overcome by the method of Nefske *et al.* [**27**] described above, but accuracy will tend to suffer because the coupled and uncoupled modes do not have quite the same shape. More recently (1998) Desmet *et al.* [**31**] have suggested that the size problem can be solved by using wave functions instead of the normal polynomial shape functions. The authors have demonstrated that, for an idealized car cabin model, the solution CPU (central processing unit) time was approximately one-thirteenth of the conventional FEM run. However, the structural model used consists of an assembly of simple flat and uniform plates, so that a predominantly flexural wave assumption is valid.

Unfortunately, for an actual car, the considerable non-uniformity of the structure makes it very difficult to predetermine the wave type which, in any case, will be mixed in an unknown way. However, a more recent paper [**32**] by Sas *et al.* claims that they have made significant progress in overcoming this

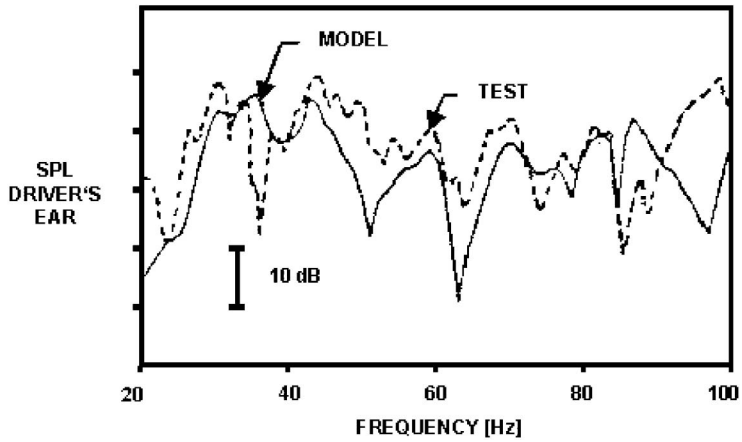

Fig. 4 Predicted versus measured sound pressure level at driver's ear. (This material has been reproduced from *International Journal of Vehicle Design*, Vol. 6, No.1, 1985. Figure 12 in Vehicle interior acoustic design using finite element methods, by D. J. Nefske and S. H. Sung, by permission of Interscience)

problem. It should also been borne in mind that recent successes in predicting vehicle interior noise using statistical energy analysis (see section 6.2 below), where similar problems exist, suggest that this is not such a large difficulty as might first appear.

There have been a number of attempts to determine whether the flexibility of the cabin walls has any significant effect. The earliest was by Jha and Priede [**1**], where they encased the cabin part of a small car in a concrete block, with a small tunnel entrance through one window. This enabled the mode shapes and natural frequencies to be measured with the certainty of rigid, hard walls. These modes were then compared with similar measurements made in the normal car. Figure 5 shows the results of this comparison.

Although the exercise was valuable, because it determined the true hard-wall natural frequencies, it is difficult to conclude much from the figure since the modal overlap factor causes the modes to merge, except at very low frequencies. This merging is particularly prevalent with the complete trimmed car because of the damping. However, it is also present with the encased car at higher frequencies, due to the rapidly increasing modal density. Nevertheless, at low frequencies there is a definite tendency for the natural frequencies to be reduced by the flexibility of the walls. This appears to be consistent with the findings of Hong and Kim [**33**], who concluded that the coupling strength is related to the ratio of mass of the acoustic medium to mass of the structural system. Kopez and Lalor [**34**] have also analysed this problem by comparing the forced acoustic response of a rectangular cavity, firstly with rigid walls and then as a fully coupled system with walls made from 1 mm thick steel sheets. Figure 6 shows the results of this analysis.

The walls are much more flexible than would be the case with a car body structure, so any flexibility effects would be much exaggerated. Nevertheless, apart from the (high-order) structural mode at 80 Hz, resonant amplitudes are not much affected. The influence on the natural frequencies is shown in Table 2. As expected by the findings of previous researchers, the flexible walls have reduced the natural frequencies, but the effect is less than 6 per cent.

Cepkauskas and Stevens [**35**] investigated this problem by analysing a one-dimensional air column with an exciting piston at one end and a spring-loaded piston at the other end. They also concluded that the coupling is related to the mass of the fluid. They found that when the first acoustic mode is excited at its natural frequency the structure can reduce the acoustic pressure amplitude by acting as a vibration absorber. Craggs [**36**], using the same model, has found that when the *in vacuo* structural and hard-wall acoustic natural frequencies are equal, the coupled acoustic mode behaves as though the structure does not exist. It should be pointed out that this analysis was carried out with zero damping and the effect will be much mitigated by the presence of damping. Nevertheless, this finding tends to be substantiated by Morrey and Whear [**37**], who claim to have found a $(\frac{1}{2}, 0, 0)$ acoustic mode in a small hatchback car. Since the rear hatch glass of that period was usually softly mounted in its frame, it is likely that a structural/

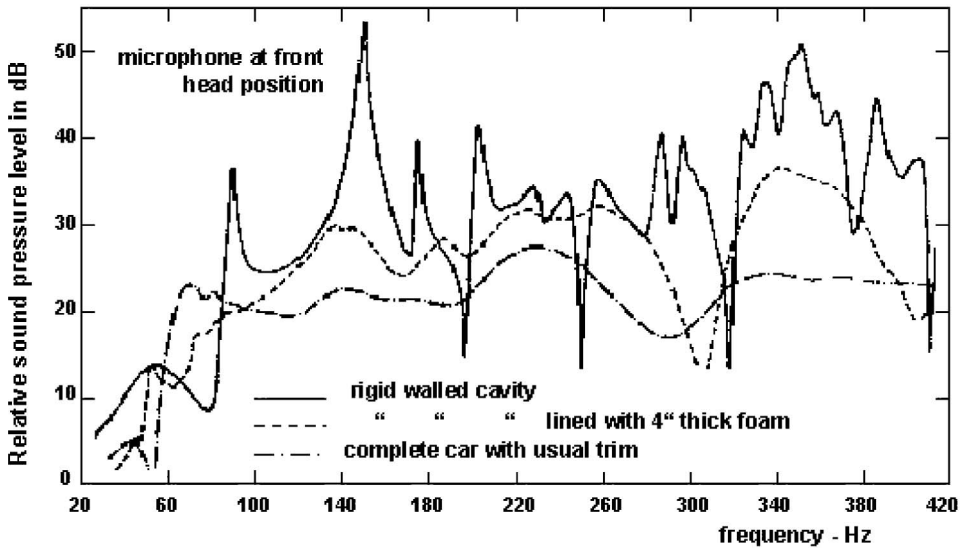

Fig. 5 Noise spectra inside car cavity (loudspeaker at front seat position)

d000000199 13-12-06 16:24:58 Rev 14.05
The Charlesworth Group, Wakefield 01924 204830

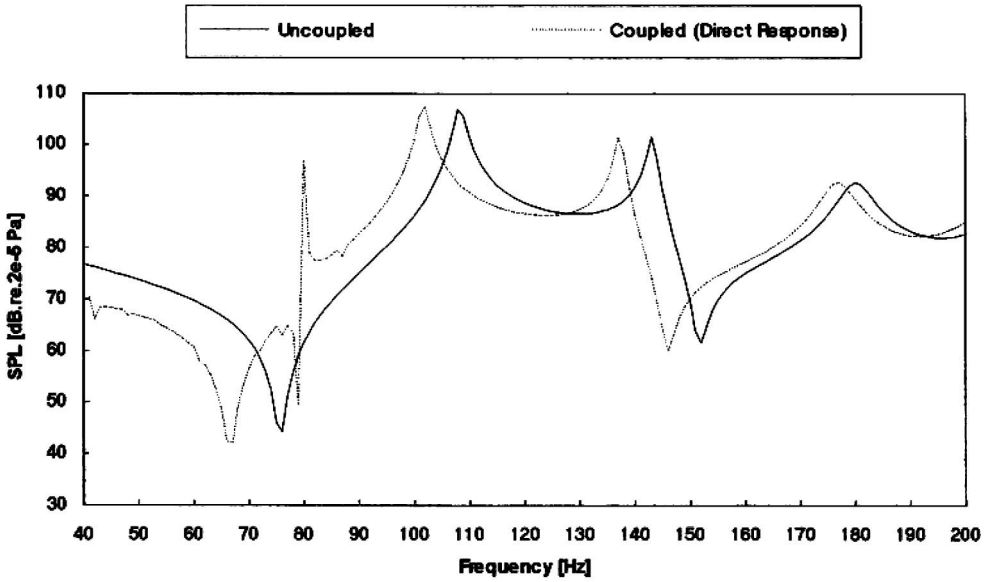

Fig. 6 Predicted sound pressure level at driver's ear position

Table 2 Coupled and uncoupled natural frequencies of acoustic cavity

		Natural frequencies (Hz)			
		Exact		BEM	
Mode number	Mode (l, m, n)	Uncoupled (rigid)	Uncoupled (rigid)	Coupled (undamped)	Coupled (undamped)
1	1, 0, 0	106	108	102	103
2	0, 1, 0	142	143	137	138
3	1, 1, 0	177	180	177	177

acoustic coincidence of natural frequencies had occurred. A more recent paper by Jayachandran *et al.* [**38**] shows that generally a flexible boundary does not affect the internal pressure distribution very much (presumably away from structural/acoustic natural frequency coincidence), but does have a very significant effect at the boundaries. As the authors point out, this is very important when attempting to predict the effect of the trim, since the normal velocity will no longer be zero with flexible walls. The 1988 Rayleigh Medal Lecture given by D. G. Crighton [**39**] gives a very comprehensive summary of the theoretical aspects of this structure/acoustic coupling issue.

The difficulties associated with the non-symmetric nature of the equations of motion with the coupled solution have been investigated by a number of researchers. Langley [**40**] uncouples the equations by including deflection terms due to the internal pressure, in the structural deflection vector, which he then calculates separately. This is quite similar to the solution proposed earlier by Nefske *et al.* [**27**], although Langley solved the equations by inverting the dynamic stiffness matrix, rather than using the modes – the vast increase in computer power over the intervening decade making this a practical alternative. Both Luo and Gea [**41**] and Sandberg and Göransson [**42**] solved the problem by making the matrices symmetric by changing the variable. The advantage of this new formulation is that it allows standard solution routines to be used. The resulting equations are

$$\begin{bmatrix} \mathbf{M}_s & 0 & 0 \\ 0 & \mathbf{K}_f & 0 \\ 0 & 0 & 0 \end{bmatrix} \cdot \begin{bmatrix} \ddot{\mathbf{U}}_s \\ \ddot{\boldsymbol{\Psi}} \\ \ddot{\mathbf{P}} \end{bmatrix} + \begin{bmatrix} \mathbf{K}_s & 0 & -\mathbf{M}_c^T \\ 0 & 0 & \mathbf{B}^T \\ -\mathbf{M}_c & \mathbf{B} & -\mathbf{M}_f \end{bmatrix} \cdot \begin{bmatrix} \mathbf{U}_s \\ \boldsymbol{\Psi} \\ \mathbf{P} \end{bmatrix} = \begin{bmatrix} \boldsymbol{L}_s \\ 0 \\ 0 \end{bmatrix}$$

where $\mathbf{U}_s$ = structural displacement, $\mathbf{P}$ = fluid pressure, $\boldsymbol{L}_s$ = load vector due to external loads on the structure,

d000000199 13-12-06 16:24:58 Rev 14.05
The Charlesworth Group, Wakefield 01924 204830

$\mathbf{M}_s$ = mass of structure, $\mathbf{K}_s$ = stiffness of structure

$$(\mathbf{K}_f)_{ij} = \rho_s \int_V \nabla N_\psi^i \nabla N_\psi^j \, dV$$

$$(\mathbf{M}_f)_{ij} = 1/(\rho_s c^2) \int_V N_P^i N_P^j \, dV$$

$$(\mathbf{M}_c)_{ij} = \int_S N_P^i N_S^i n \, dS$$

$$(\mathbf{B})_{ij} = \int_V \nabla N_P^i \nabla N_\psi^j \, dV$$

where ψ = fluid displacement and N = shape function.

At this stage, historically, it appeared that quite reasonable predictions of internal noise could be made using a finite element model of both the structure and the cabin air space, provided no trim or seats were present. In fact, even today, many company engineers are using uncoupled FE models, with empirical damping values to allow for the effect of the trim, for noise vibration harshness (NVH) development. A fairly recent example of this is given in a paper by Turner and Turgay [**43**]. Campbell *et al.* [**44**] have treated the trim damping in a similar way but have also allowed for the seats by treating them as solid boundaries. However, they have also performed the coupled computation, using the method proposed by Nefske *et al.* [**27**]. Nevertheless, for an accurate absolute prediction, it was now clear that it would be necessary to use a coupled model that was also able to predict the effect of the trim. Subsequently, many papers, in addition to those already mentioned in connection with aircraft noise, have been published on this latter aspect. Tinti and Scaffidi [**45**] describe an experimental method for determining the relevant acoustic parameters for a metal panel covered with typical trim material. However, Craggs [**46**] presents a simple theory for including absorption material characteristics into the noise prediction model, which is specifically aimed at the lower order acoustic modes. On the other hand, Hong and Kim [**47**] have conducted an in-depth analytical study on the effects that the absorbing materials have on system response. Taking a more pragmatic approach, Sung *et al.* [**48**] have obtained excellent predictive accuracy (see Fig. 8 later) by simulating the structural dynamic effect of the trim by adding mass. They also allowed for the seats by modelling them from acoustic elements but with a mass density 10 times that of air. Several other researchers have treated the seats in this way, e.g. Stokes *et al.* [**49**]. However, Qian and VanBuskirk [**50**] have also accounted for the porosity of the seats. One particularly difficult aspect of seat modelling is when the back seat also forms the partition between the passenger cabin and the luggage boot. This has been investigated by Campbell *et al.* [**44**] and by Kopuz and Lalor [**51**]. The latter researchers found that the porosity of the seat and the hole size in the supporting frame have very significant effects on the cabin noise spectrum.

When all the above refinements are applied to a coupled structure/acoustic FE model of a car, the accuracy of prediction can be very good. Figure 7, reproduced from reference [**48**], probably represents the best that can be achieved as far as FE prediction of internal noise is concerned. The figure shows that, apart from a few frequency ranges, prediction accuracy is generally within ± 5 dB, i.e. within the likely scatter band of actual vehicles.

Although somewhat outside the scope of this paper, it is worthwhile briefly describing the main techniques used for solving the very large number of equations (frequently well in excess of one million) generated by these FE models. There are basically two methods: direct and modal superposition. These both start with the equation of motion in its harmonic form

$$[-\omega^2 \cdot \mathbf{M} + j\omega \cdot \mathbf{C} + \mathbf{K}] \cdot \{\boldsymbol{X}\} = \{\boldsymbol{F}\}$$

where $\mathbf{M}$ = mass matrix, $\mathbf{C}$ = viscous damping matrix, $\mathbf{K}$ = stiffness matrix, $\boldsymbol{X}$ = displacement amplitude vector, and $\boldsymbol{F}$ = force amplitude vector. With the direct method, $\{\boldsymbol{F}\}$ is premultiplied by the inverse of $[-\omega^2 \cdot \mathbf{M} + j\omega \cdot \mathbf{C} + \mathbf{K}]$ at each frequency (ω) of interest

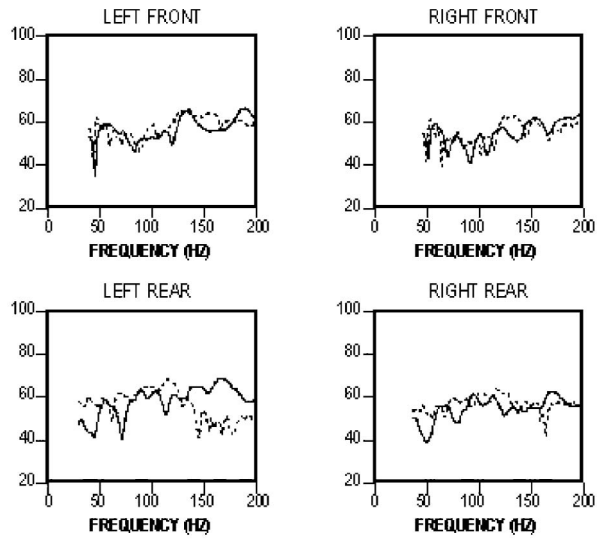

Fig. 7 Comparison of predicted and measured sound pressure level at occupant ear locations (--- predicted, ··· measured). (Reprinted with permission from SAE paper 991798 © 1999 SAE International)

d000000199 13-12-06 16:24:58 Rev 14.05
The Charlesworth Group, Wakefield 01924 204830

to directly obtain a spectrum of $\{\boldsymbol{X}\}$. Although this involves many inversions of a very large matrix, its narrow-banded nature, together with the use of modern approximate inversion techniques, have somewhat alleviated this problem.

The first step with the modal superposition method is to obtain the eigenvalues and eigenvectors for the undamped model. The eigenvectors are then used to diagonalize the [**M**], [**C**], and [**K**] matrices. This transforms the above equation of motion into a series of equations, each of which only contains a single variable x_i. Thus, all the elements of $\{\boldsymbol{X}\}$ (i.e. $\{x_1, \ldots, x_i, \ldots, x_N\}^{\mathrm{T}}$) can be solved directly. One way of carrying out this method on relatively low-capacity machines is to use substructuring. Here, the model is split into a number of smaller parts which are then solved independently. These independent solutions are then combined to form the complete solution. One problem with this is that retention of the boundary degrees of freedom around each substructure significantly increases computer run-times. However, one way of overcoming this is by a very recent development [**52**–**54**] termed 'automated multilevel substructuring' (AMLS), where the FE model is automatically divided into many substructures. The model is then transformed so that its response is represented in terms of the substructure eigenvectors. Reference [**53**] also gives a fairly detailed account of the direct and modal superposition methods, in addition to AMLS. Both references show that, even with car body models of well over two million degrees of freedom, CPU and turnround times are shorter on a single processor workstation using AMLS than on a multiprocessor supercomputer using the more conventional modal superposition technique. Further refinements of this technique are described in references [**55**] and [**56**].

Although there are many researchers who prefer to continue using a purely FE model, a growing number are opting for a mixed model. With this the structural part is computed using the FEM and the internal acoustics part using the BEM. Because the theory of the BEM is not widely understood, a brief description of the method, as applied to the acoustics of a passenger cabin, is given here. The BEM is based on an integral transformation of the Helmholtz equation, i.e. the so-called boundary integral equation [**57**], which relates the pressure (P_α) at a point α anywhere in the fluid (air) and the pressure (P_β) and normal pressure gradient ($\partial P_\beta / \partial n$) at a point β anywhere on the surface

$$C_\alpha P_\alpha + \frac{1}{2\pi} \int_S P_\beta \frac{\partial}{\partial n}\left(\frac{\mathrm{e}^{-\mathrm{j}kr}}{r}\right) \mathrm{d}S = \frac{1}{2\pi} \int_S \frac{\partial P_\beta}{\partial n} \frac{\mathrm{e}^{-\mathrm{j}kr}}{r} \mathrm{d}S$$

where $C_\alpha = 0$ (α outside the field), $= 1$ (α on the boundary), $= 2$ (α inside the field), $S =$ the surface area of the boundary, $k =$ the wave number, and $r =$ the distance between α and β.

The outer surface (cabin walls) of the acoustic space is meshed with nodes and small elements, as with a finite element model (see Fig. 11, given later for an example). The way in which the acoustic pressure and normal pressure gradient at the surface vary over each element is assumed to follow a simple mathematical law (shape function), which is related to their values at the nodes. Since α can be anywhere in the fluid, it can also be on the boundary surface. Suppose, for example, that α is at node 1. The above boundary integral equation is evaluated for each element in turn by inserting the appropriate shape functions. Each of the two total surface integrals in the equation is then equal to the sum of the associated elemental integrals

$$\int_S = \int_{el.1} + \int_{el.2} + \cdots + \int_{el.N}$$

Thus, for node 1, the boundary integral equation becomes

$$C_\alpha P_1 + f_1(P_1, P_2, \ldots, P_N) = g_1\left(\frac{\partial P_1}{\partial n}, \frac{\partial P_2}{\partial n}, \ldots, \frac{\partial P_N}{\partial n}\right)$$

or

$$(a_{11}, a_{12}, \ldots, a_{1N}) \begin{Bmatrix} P_1 \\ \vdots \\ P_N \end{Bmatrix} = (b_{11}, b_{12}, \ldots, b_{1N}) \begin{Bmatrix} \partial P_1/\partial n \\ \vdots \\ \partial P_N/\partial n \end{Bmatrix}$$

Thus α is assumed to be at all the other nodes in turn. This produces N equations which can be combined to give

$$[\mathbf{A}] \begin{Bmatrix} P_1 \\ \vdots \\ P_N \end{Bmatrix} = [\mathbf{B}] \begin{Bmatrix} \partial P_1/\partial n \\ \vdots \\ \partial P_N/\partial n \end{Bmatrix}$$

Because there are $2N$ unknowns and only N equations, a total of N boundary conditions (consisting of known values of P_i and/or $\partial P_i / \partial n$) must be supplied as input data. The solution then enables the pressure and/or the pressure gradient at all nodes (and between nodes, because of the shape functions) to be obtained. Because k is frequency dependent the above procedure must be carried out at a single frequency. It

d000000199 13-12-06 16:24:58 Rev 14.05
The Charlesworth Group, Wakefield 01924 204830

is then repeated at all other required frequencies. Reference [**58**] gives a straightforward explanation of how the method is applied to vehicle interior noise problems.

Although not the originators of the BEM concept, in 1984 Sestieri *et al.* [**17**] published a paper showing the application to cavity noise problems. A year later, Sestieri developed the concept in more detail [**59**]. A similar analysis was reported by Succi [**60**] in 1987. The next development was verification of the BEM theory by comparing measured noise at a point within an enclosure with predictions using measured boundary surface velocities as input to the BEM model of the acoustic space. Coyette and McCulloch [**61**], Hussain [**62**], Marburg [**63**], and Katsuta *et al.* [**64**] are examples of researchers who have carried out this exercise. Actually, agreement with experimental values is rather poor except for the results by Coyette and McCulloch [**61**], which are reproduced below in Fig. 8.

In this case the experimental results were carried out on a scale model (probably quarter scale) of a car cabin, so the above frequencies should be divided by four for comparison with an actual car. Agreement is quite good at low frequencies and the authors state that the increasing error with frequency is due to the coarse mesh used for the model. No explanation is given for the frequency shift. This last paper [**61**] also gives a very useful table that highlights the essential features of the FEM and the variational and direct BE methods, which is reproduced below as Table 3.

Apart from most of the authors of the BEM-related papers already cited, many others have written about general aspects of the theory. These include Cheng and Seybert [**65**], Utsuno and Inoue [**66**], Suzuki *et al.* [**67**], Sorokin [**68**], and Soenarko and Seybert [**69**]. As with the FE models previously described, the structure/acoustic coupling problem is another aspect of the application of the BEM that has received much attention in recent years. Researchers investigating this problem include Cousins and Goodman [**70**], Franchek and Bernhard [**71**], Slepyan and Sorokin [**72**], Sorokin [**73**], Everstine [**74**], and Chen *et al.* [**75**]. Urushiyama and Nomoto [**76**] used measured vibration results as input to the BEM model but then employed it to find the best place to put the trim. Suzuki *et al.* [**58**] showed how to allow for absorbent trim on the walls and openings, such as the sunroof. By the mid 1990s, experience with FEM (structural) models coupled with BEM acoustic models had reached the point where realistic predictions of actual vehicles could be made. Good fairly recent examples of this are given in papers by Seybert *et al.* [**77**] and Hargreaves [**78**]. Seybert *et al.* [**77**] give a detailed account of their prediction of the internal noise of a tractor cab with both mechanical (shaker) and air-borne (loudspeaker) excitation. Figure 9 gives their overall view of the possible methodologies that can be used for this task although, for the results presented below, they actually used a BEM model of the cab interior.

The FEM model of the cab structure used by the authors is shown in Fig. 10. Shell elements are used for the panels and beam elements for the supporting frame. Point mass elements are also used to represent the steering column and seat. The model has a total of 50 000 degrees of freedom although, as the authors point out, even cab models (much simpler than that of a car body shell) are often much larger. The BEM model of the interior is shown in Fig. 11.

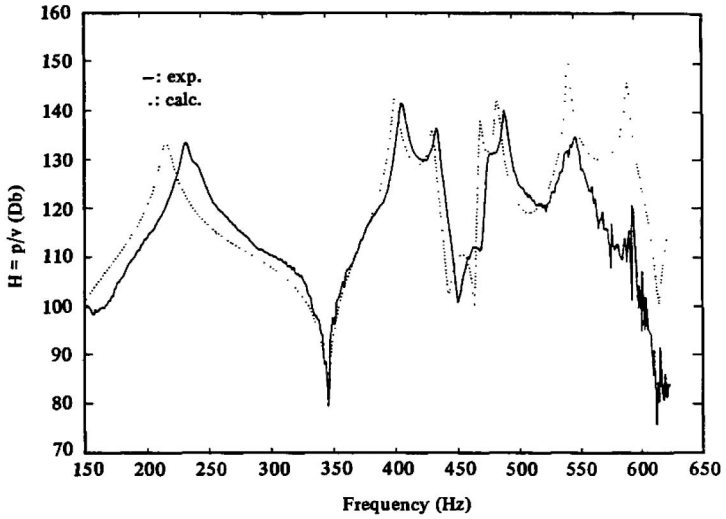

Fig. 8 Frequency response function, experiment versus calculation

d000000199 13-12-06 16:24:58 Rev 14.05
The Charlesworth Group, Wakefield 01924 204830

Table 3 Comparison of modelling capabilities. (This material has been reproduced from *Autotech '89, Noise Refinement: Design and Analysis* (C399/21). Modelling interior and exterior acoustics using finite element and boundary element methods, Table 1, by J. Coyette, K. R. Fyfe and C. F. McCulloch by permission of the Council of the Institution of Mechanical Engineers)

Feature	FE	BE variational	BE direct
Mesh requirement	Domain	Boundary	Boundary
Meshing speed	Slow	Fast	Fast
CPU time	Short	Long	Moderate
Matrix mix	Banded/symmetric	Full/symmetric	Full/unsymmetric
Easy structural coupling	Good	Good	Fair
Direct response	×	×	×
Eigenmodes	×		×
Interior fields	×	×	×
Exterior fields		×	×
Simultaneous interior/exterior		×	
Sources	×	×	×
Scattering	×	×	×
Baffles		×	×
Half-space		×	×
Surface inpedance	×	×	×
Absorbers (volume)	×		
Transfer impedance	×		
Surface acoustic variables	×		×
Field acoustic variables	×	×	×
Planar symmetry	×	×	×
Axisymmetry	×		×

× indicates that the capability exists.

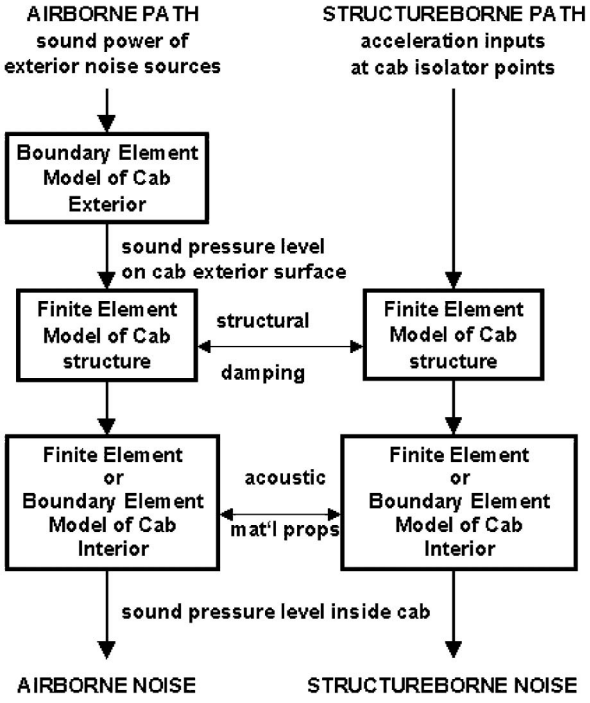

Fig. 9 Interior noise prediction process model. (Reprinted with permission from SAE paper 971955 © 1997 SAE International)

Although actually created from the FEM model, it has a much courser mesh. This is made possible because the acoustic wavelengths are much shorter than the structural wavelengths at low frequencies.

Fig. 10 Finite element model of the cab. (Reprinted with permission from SAE paper 971955 © 1997 SAE International)

The reason for keeping the BEM model as small as possible is that the matrices [**A**] and [**B**] involved in the governing equations

$$[\mathbf{A}]\text{–}\{\boldsymbol{P}\} = [\mathbf{B}]\cdot\{\partial P/\partial n\}$$

are fully populated (each point acoustic source on the surface has an influence on every other point). Thus the solution time required increases very rapidly with size. Figure 12 shows the comparison between measured and predicted sound pressure at an

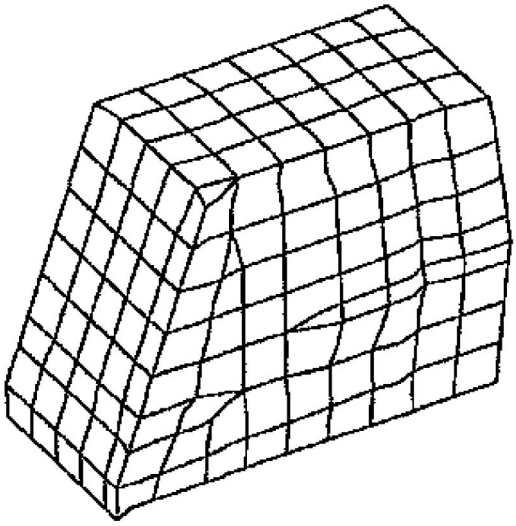

Fig. 11 Boundary element mesh of the cab. (Reprinted with permission from SAE paper 971955 © 1997 SAE International)

interior point, when the cab was only excited by a shaker.

It can be seen that excellent agreement has been achieved up to at least 500 Hz. Of course, this level of agreement has been achieved mainly because the structure is much simpler than that of a car, and there is little or no trim. In addition, measured damping values were input to the model. In a later paper (1994), McCulloch and Coyette [**79**] argue that the FEM has certain advantages over the BEM for interior acoustics because it allows inhomogeneous fluids and volume absorbent effects. This enables seats and multilayer absorbent/damping trim to be realistically modelled. Cheng [**80**], in his PhD Thesis (1994), gives a reasonably comprehensive assessment of both the FEM and the BEM techniques.

An interesting variation of the BEM technique has recently been developed by Desmet [**81**]. This is the wave-based method (WBM), which is also based on the underlying Helmholtz equation. With this method the dynamic acoustic field is approximately represented by wave functions that are exact solutions of the Helmholtz equation. Pluymers *et al.* [**82**] show that the WBM exhibits a higher convergence rate than the FEM so can therefore be used up to higher frequencies. Van Hal *et al.* [**83**] show how the FEM can be coupled to the WBM to produce a hybrid acoustic model. This enables the geometrical flexibility of the FEM to be combined with the computational efficiency of the WBM.

To conclude this assessment of FEM/BEM modelling, Fig. 13, which has been reproduced from reference [**49**], shows a more detailed procedure flowchart for use with this methodology.

6.2 Statistical energy analysis (SEA) method

Because energy accountancy/power flow methods [**18**, **19**] are essentially the same as statistical energy analysis, as shown by Lyon [**84**], they are included under this heading. SEA was devised in the late 1950s because the current computer power was

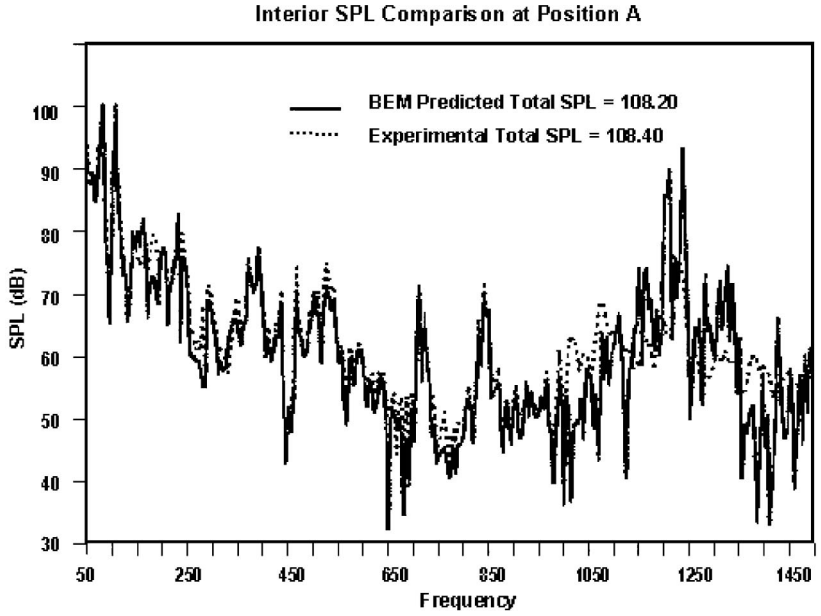

Fig. 12 Comparison between measured and predicted sound pressure level inside of the cab. (Reprinted with permission from SAE paper 971955 © 1997 SAE International)

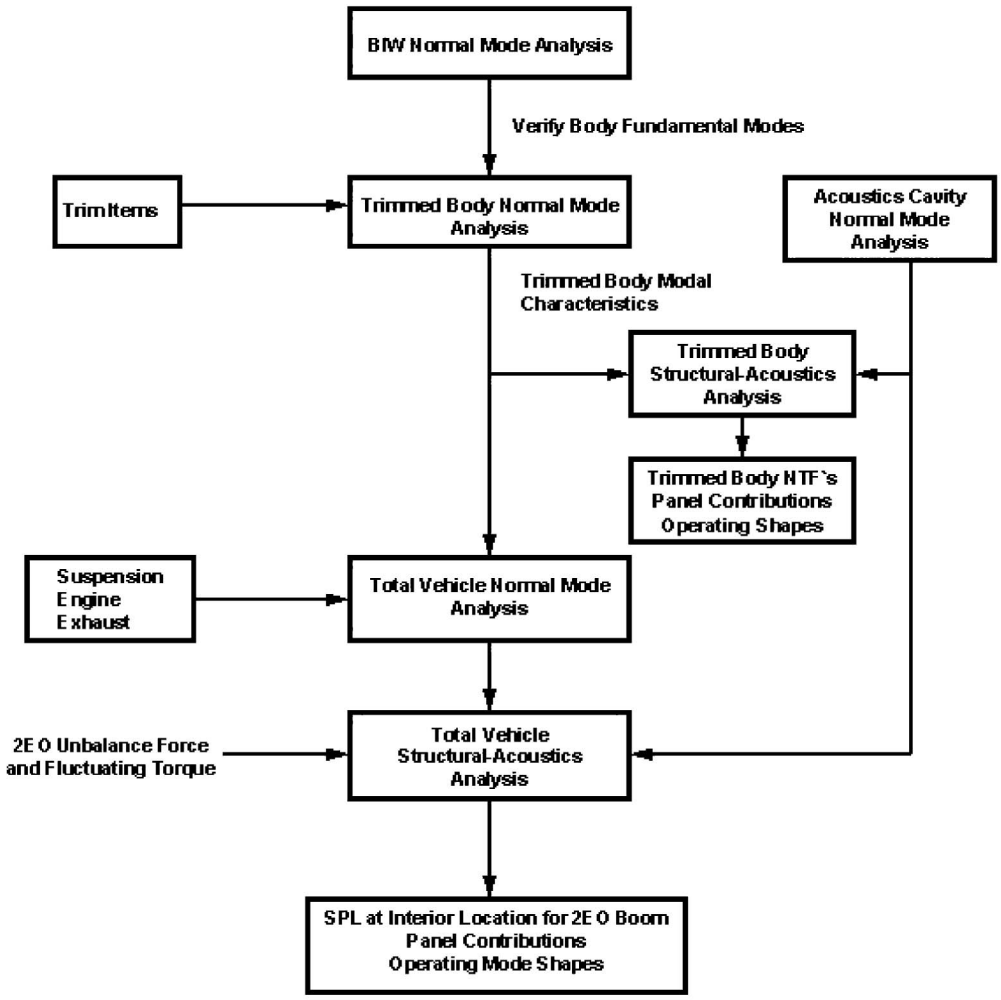

Fig. 13 Structural–acoustic analysis process. (Reprinted with permission from SAE paper 971914 © 1997 SAE International)

not sufficient to predict stress levels on the new generation of spacecraft by the traditional modal techniques. The aerospace industry has continued to use SEA, in addition to the FEM, up to the present time because it is particularly well suited to random vibration problems. SEA is also well suited to analysing aircraft and rocket structures because they are relatively simple in shape (e.g. rib-stiffened cylinders). In contrast to this, prior to the mid 1980s, nearly all researchers connected with the automotive industry only used the new FE methods that they had learnt from the aerospace industry. However, the increasing complexity and cost of these models (in a much more cost-conscious industry), together with the need to consider high frequencies for noise quality reasons, led the automotive researchers to have another look at SEA. Although SEA was first envisaged as a high-frequency technique, in recent years there have been increasing attempts to apply it to lower frequency problems.

The basic SEA concept is very simple. The system under consideration, say a car, is split up into subsystems, e.g. a car roof (structural subsystem) and passenger compartment (acoustic subsystem). Each subsystem (an experimentally based car model would typically contain about 50 subsystems) is characterized by its internal loss factor (η_i), its coupling loss factors (η_{ij}), which determine the efficiency by which it can transmit vibrational power to its neighbours, and its internal energy (E_i). If power from an external source is input to a subsystem, some of it will be dissipated within that subsystem due to its damping and the rest will be transferred to the neighbouring subsystems. By applying this principle to each subsystem in turn, a series of power balance equations are built up

$$[\mathbf{P}] = \omega[\mathbf{L}]\cdot[\mathbf{E}]$$

where $[\mathbf{P}]$ = a column matrix of input powers, $[\mathbf{L}]$ = a square matrix consisting of internal loss factors and

coupling loss factors, and [**E**] = a column matrix of the subsystem energies. These quantities are averages over frequency bands (usually one-third octave), so ω = the centre (circular) frequency of the band under consideration. The above power balance equation is thus three-dimensional, with each vertical 'layer' representing the quantities appropriate to one particular (one-third octave) band.

Once the elements of [**L**] have been determined (empirically and/or theoretically), [**E**] can be calculated for known input powers [**P**]. The space-averaged vibration velocities ($\langle v^2 \rangle$) of each structure and/or the space-averaged sound pressures ($\langle p^2 \rangle$) of each acoustic cavity can then be found from:

$$E_{\text{structure}} = m\langle v^2 \rangle \qquad \text{and} \qquad E_{\text{acoustic}} = V\langle p^2 \rangle / (\rho c^2)$$

where m = subsystem mass, V = subsystem volume, ρ = air density, and c = speed of sound in air.

One of the first papers to be published on the application of SEA to car internal noise was by DeJong [**85**] in 1985. He used software that employs simple structural and acoustic subsystems (e.g. plate, beam, cylinder, rectangular cavity) for which there are closed-form analytical expressions for the required coupling loss factors. Although most of his predictions are within 5 dB of the measured values (630 to 2000 Hz), he chose load cases where only one excitation source was dominant (this reduces the problem to a relatively simple case) and it is not clear to what extent he used empirical values as input. Nevertheless, it was an interesting attempt at noise prediction and stimulated many other researchers to consider SEA as a predictive tool. In parallel with these applied developments, others examined the limitations of the SEA theory to see if its scope could be extended to lower frequencies. Of particular importance in this respect is a paper published in 1987 by Keane and Price [**86**] in which they modified the existing SEA theory so that it can cater for strongly coupled subsystems. Although, unfortunately, there is no closed-form solution for their equations except in simple cases, they have demonstrated that the weak coupling assumption can be relaxed provided there are plenty of modes and that the exciting forces are incoherent. Craik *et al.* [**87**] have examined the confidence limits when SEA is applied at low frequencies, where the modal density is low. However, Plunt [**88**] has warned against the misuse of SEA and has enumerated some of its limitations. Fredö [**89**] has suggested that prediction accuracy could be improved if indirect couplings (i.e. SEA links between subsystems not physically joined) are included in the model. Some of these developments are beginning to be incorporated into the modern SEA software packages that are now extensively used in the industry. Of particular interest from a practical point of view is the ability of SEA to accurately predict (generally within a couple of dBs from 100 Hz to 10 kHz) the sound transmission loss through a trimmed panel, even when it contains some holes. Cimerman *et al.* [**90**], Powell *et al.* [**91**], and Liu *et al.* [**92**] have all published papers on this topic, and the first of these also includes the effect of acoustic absorption. Onsay and Akanda [**93**] have published a detailed model to predict structure-borne noise from the road. Dong *et al.* [**94**] have shown that the combined structure-borne and air-borne interior noise due to road inputs can be predicted to within 2–4 dB over the 200 Hz to 3 kHz frequency range. Figure 14, taken from reference [**7**], shows how accurately road noise can now be predicted. However, there is still a certain amount of empirical input involved.

A paper by Parrett *et al.* [**95**] explains in detail how a hybrid theoretical/experimental model is constructed. Some of the theoretical models can be very large (with several hundred subsystems) and Moore *et al.* [**96**] has shown how they can be condensed in size to make them comparable with experimental versions. A number of researchers have developed methods for validating theoretical models. Moeller *et al.* [**97**] use a thermal analogy, Chen *et al.* [**98**] and Wang *et al.* [**99**] both use artificial excitation, and Manning [**100**] uses modal power. Hermans and Iadevaia [**101**] give general guidelines for experimental SEA.

One of the problems associated with predicting low-frequency internal car noise with SEA is that the passenger cabin has very few modes in this region. Modal densities have been calculated by Sung

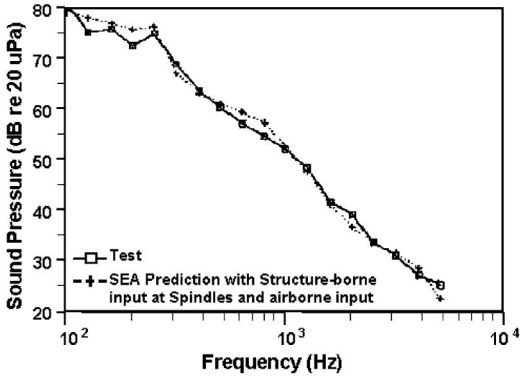

Fig. 14 Sound pressure at the driver's head. (Reprinted with permission from SAE paper 971972 © 1997 SAE International)

d000000199 13-12-06 16:24:58 Rev 14.05
The Charlesworth Group, Wakefield 01924 204830

et al. [**48**] for a fully trimmed car and Fig. 15 shows the mode count as a function of frequency, taken from this paper.

It can be seen that, although both the structural and acoustic mode counts are rising rapidly with frequency, the modal density of the acoustic space is approximately 1/30 that of the structure. This means that not only is the uncertainty of prediction increasing rapidly as frequency is reduced (see Fig. 14) but it is also difficult to subdivide the cabin space into smaller subsystems (to show the spatial variation of sound pressure). One way out of this difficulty might be to treat the cabin walls as free-field radiators into the near field (see comments in relation to Fig. 2). This is unlikely to be valid in the reverberant range below about 200 Hz, but might be a solution above that frequency. Papers by Beissner [**102**] and Nolte and Gaul [**103**] give in-depth analyses of acoustic radiation to the near field. This low-frequency problem also occurs with vibration prediction, and this is well illustrated in a paper by Steel [**104**]. Figure 16, reproduced from his paper, shows this discrepancy quite clearly.

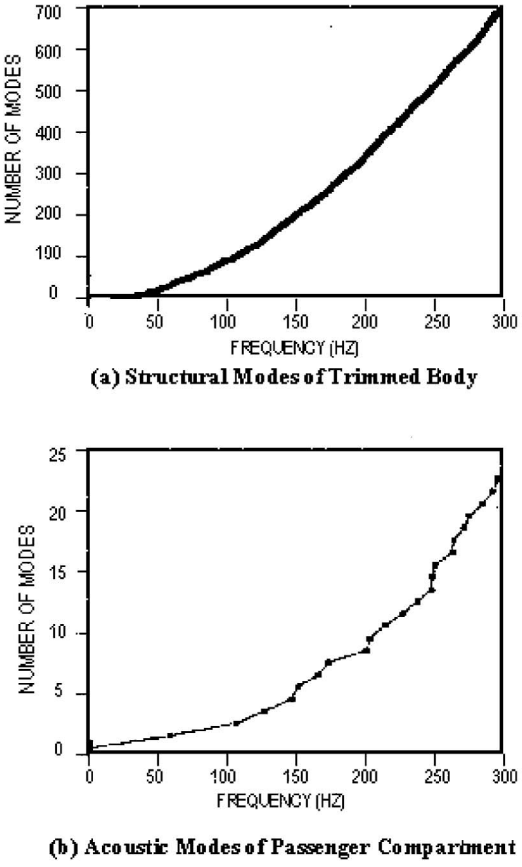

Fig. 15 Computed structural and acoustic modes. (Reprinted with permission from SAE paper 991798 © 1999 SAE International)

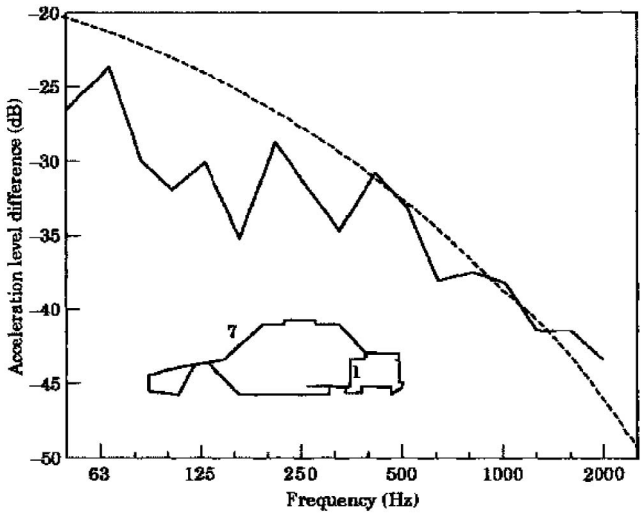

Fig. 16 The measured and predicted acceleration level difference for transmission from the boot panel to the windscreen (such as 1 to 7) (--- measured, ··· Predicted). (Reprinted from *Journal of Sound and Vibration*, Vol. 193, No. 3, 1996, J. A. Steel, 'Prediction of structural vibration transmission through a motor vehicle using Statistical Energy Analysis', pp. 691, Fig. 5 © 1996, with permission from Elsevier Science)

The model used here was somewhat courser in detail compared with the industrial models described above, so the effect will be a little exaggerated. Also, the distance between the input and output is almost the complete length of the car, so the test is quite severe. Nevertheless, it is quite clear that there is a low-frequency problem. Moeller and Powell [**105**] have presented a paper that reviews the application of SEA to the automotive industry. An example of the statistical analysis of prediction errors, using an SEA model, is given in a recent paper by Langley and Brown [**106**].

Another interesting development in this category is energy finite element analysis (EFEA). With this technique the energy flow through a structural/acoustic system is assumed to follow a thermal analogy; i.e. the governing differential equation is

$$-c^2/(\eta\omega)\nabla^2\langle e\rangle + \eta\omega\langle e\rangle = \langle \pi_{\text{in}}\rangle$$

where c = structural wavespeed, ω = cyclic frequency, η = loss factor, $\langle e\rangle$ = average energy density, and $\langle \pi_{\text{in}}\rangle$ = average power input. The element matrices are formulated in the same way as with the FEM except that the variables are now energy and power rather than deflection and force. Although not the originator of the idea, Bernhard has pioneered the application to automotive structural/acoustic problems and a paper by Bitsie and Bernhard [**107**] outlines the

technique. Gur *et al.* [**108**] have also published a paper on the subject. At present the technique has only been demonstrated on relatively simple systems and it appears that it is not yet at the stage where it can be used to predict car interior noise accurately.

6.3 Hybrid methods

One possible way to model the structural/acoustic coupling problem is to consider that the vibration of the structure is diffuse and that the interior acoustics is deterministic. In order to test the appropriateness of this hypothesis, Bonilha and Fahy [**109**] have investigated the diffuseness of a car body shell. They showed that, although the structure is diffuse at high frequencies, it becomes progressively less so as frequency is reduced. Figure 17, which has been reproduced from their paper, demonstrates that the structure cannot be considered diffuse at a frequency as low as 315 Hz, particularly with mechanical excitation (which is the most likely excitation at these low frequencies).

The figure shows the correlation coefficient between two points on the roof, $r(m)$ apart. The 'theory' curve is calculated with the assumption that the vibrational field is diffuse. In his PhD Thesis, Bonilha [**110**] has studied this application in some depth, but it does not appear that the technique has any advantage over the more conventional SEA method.

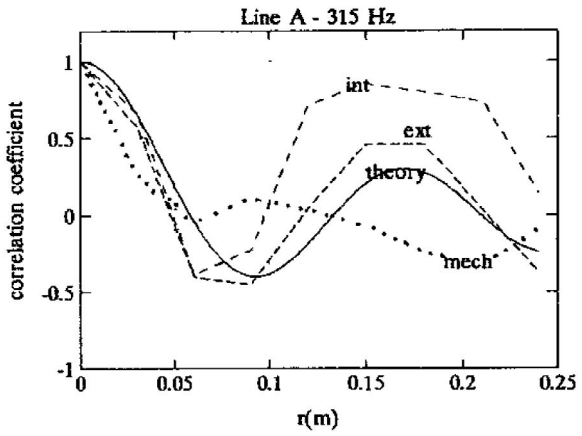

Fig. 17 Comparison of roof correlation coefficients at line A obtained with different types of excitation, 315 Hz (one-third octave band) (- - - internal acoustic excitation, --- external acoustic excitation, ⋯ mechanical excitation, --- diffuse wave field), where $r(m)$ = distance (m) along a line from the centre of the roof towards the front. (Reprinted from *Applied Acoustics*, Vol. 43, 1994, p. 1, Bonilha *et al.* 'Measurements of vibration field correlation on a car body shell', Figure 10 © 1994, with permission from Elsevier Science)

However, a more recent hybrid technique has been developed to cater for situations where the structure consists of a load-carrying frame with essentially non-stressed panels attached. The global response of the frame is calculated and the resultant vibration is then considered as input to the panels at their attachment points. The frame response can be computed using an FEM model and the panel response, having a much higher modal density, by using SEA. Heidari and Marshall [**111**] have published a short paper on the subject but it is Langley and Bremner [**112**] who have published the detailed theory, including the effect of the coupling terms. In the latter authors' work the distinction between the global and the local parts of a structure is made only on the basis of wavelength. Having subdivided the complete structure in this way, the governing equations of motion are partitioned into global (g) and local (l) components, viz.

$$\begin{bmatrix} \mathbf{D}_{gg} & \mathbf{D}_{gl} \\ \mathbf{D}_{gl}^{T} & \mathbf{D}_{ll} \end{bmatrix} \begin{Bmatrix} \boldsymbol{q}_g \\ \boldsymbol{q}_l \end{Bmatrix} = \begin{Bmatrix} \mathbf{F}_g \\ \mathbf{F}_l \end{Bmatrix}$$

where $\mathbf{D}$ = the dynamic stiffness matrix, $\mathbf{D}_{gl}^{T}$ = the transpose of $\mathbf{D}_{gl}$, $\boldsymbol{q}$ = the generalized displacements, and $\boldsymbol{F}$ = the generalized exciting forces. Without loss of generality, the global coordinates $\boldsymbol{q}_g$ can be selected (or transformed) so that the matrix partition $\mathbf{D}_{gg}$ is diagonal. In this case the global admissible functions $\phi_g(x)$ can be interpreted as 'global modes', although it should be noted that the true modes of the system cannot be modelled solely in terms of $\boldsymbol{q}_g$ but also require a contribution from $\boldsymbol{q}_l$. The matrix partition $\mathbf{D}_{gl}$ governs the coupling between the global and local degrees of freedom. It is assumed that each local admissible function $\phi_l(x)$ is identified with a single subsystem, so that it is everywhere zero except within this subsystem. This enables $\mathbf{D}_{gl}$ to be expressed as

$$\mathbf{D}_{gl} \approx -\omega^2 \cdot \mathbf{M}_{gl}$$

where $\mathbf{M}_{gl}$ = the appropriate partition of the mass matrix, $\mathbf{M}$.

Now the partitioned governing equations given above can be expanded to yield

$$(\mathbf{D}_{gg} - \mathbf{D}_{gl} \cdot \mathbf{D}_{ll}^{-1} \cdot \mathbf{D}_{gl}^{T}) \cdot \boldsymbol{q}_g = \boldsymbol{F}_g - \mathbf{D}_{gl} \cdot \mathbf{D}_{ll}^{-1} \cdot \boldsymbol{F}_l$$

$$\mathbf{D}_{ll} \cdot \boldsymbol{q}_l = \boldsymbol{F}_l - \mathbf{D}_{gl}^{T} \cdot \boldsymbol{q}_g$$

The first of the above two equations can be considered as the global equation of motion. The term $\mathbf{D}_{gl} \cdot \mathbf{D}_{ll}^{-1} \cdot \mathbf{D}_{gl}^{T}$ on the left-hand side represents the influence of the local systems on the global dynamic stiffness matrix. The term $\mathbf{D}_{gl} \cdot \mathbf{D}_{ll}^{-1} \cdot \boldsymbol{F}_l$ on the right-hand side represents the influence of the local systems on the global exciting forces. The second

d000000199 13-12-06 16:24:58 Rev 14.05
The Charlesworth Group, Wakefield 01924 204830

equation represents the local equation of motion. The authors show that the mn^{th} term of $\mathbf{D}_{\text{gl}} \cdot \mathbf{D}_{\text{ll}}^{-1} \cdot \mathbf{D}_{\text{gl}}^{\text{T}}$ can be expressed as

$$(\mathbf{D}_{\text{gl}} \cdot \mathbf{D}_{\text{ll}}^{-1} \cdot \mathbf{D}_{\text{gl}}^{\text{T}})_{mn} = \omega^4 \sum_{r=1}^{N_s} \sum_{k=1}^{N_r} j_{rmn}^2(k)[(\omega_k^r)^2(1 + i\eta_k^r) - \omega^2]^{-1}$$

where j = joint acceptance function between the global coordinates and the local modes in subsystem r. The complete system contains N_s subsystems and subsystem r has N_r modes and ω_k^r and η_k^r represent the natural frequency and loss factor of local mode k of subsystem r. The authors then go on to show that

$$|(\mathbf{D}_{\text{gl}} \cdot \mathbf{D}_{\text{ll}}^{-1} \cdot \boldsymbol{F}_{\text{l}})_m|^2 = \sum_{r=1}^{N_s} \langle |Fl_{j(k,r)}|^2 \rangle_k \left\{ \langle j_{rmn}^2 / 2\eta_k^r \rangle_k \omega \pi \nu_r + \sum_{k=1}^{N_r} j_{rmn}^2(k) \right\}$$

where $\langle\rangle_k$ denotes an average over the local modes.

By substituting these expressions into the global equation of motion, the response $\boldsymbol{q}_{\text{g}}$ to known global forces $\boldsymbol{F}_{\text{g}}$ can be evaluated and $\boldsymbol{q}_{\text{g}}$ can then be substituted into the local equation of motion to obtain the local response $\boldsymbol{q}_{\text{l}}$. It should be noted that the influence of the local systems on the global system is only expressed in terms of the band-averaged properties of the local systems, so a precise deterministic description of them is not required.

The basic idea behind the possible application of this technique to the prediction of interior noise in cars is that the stiff parts of the body shell (and possibly the cabin acoustic modes) could be considered as the global system and the rest as the local system. Although this appears to have considerable potential and is understood to have already given promising results with helicopter noise, its application to the automotive problem is problematical. One of the main difficulties is likely to be the identification of which parts should be considered global and which should be considered local.

A simplified version of the above technique has been proposed by Grice [**113**]. As with the previous method, the complete structure is first divided up into stiff, long-wavelength parts (referred to as the 'spine') and flexible, short-wavelength parts (referred to as the 'receivers'). Grice shows that the long waves travelling in the spine control both the power input and the power transmission through the structure. These long waves also generate short waves in the receivers at the interconnecting junctions. Because of the large difference in wavelength between the spine and the receivers, the receivers present a locally reacting impedance to the spine. This concept is implemented in practice by modelling the spine in isolation of the receivers using the FEM. The receivers are modelled in isolation of the spine using analytical impedances. As an example of how a receiver impedance is modelled, consider a thin, flat plate (receiver) to which a beam (spine) is attached. Firstly, an infinite beam attached to an infinite plate is considered. Provided that the wavenumber k_{p} of the plate $\gg$ wavenumber k_{b} of the beam, the line impedance $\tilde{Z}'_{\text{p}}$ of the plate per unit length of the beam can be simply expressed as

$$\tilde{Z}'_{\text{p}} = \frac{2m''_{\text{p}}\omega}{k_{\text{p}}}(1 + j)$$

where m''_{p} = mass per unit area of the plate. In fact, experimental tests have shown that this is valid provided $k_{\text{p}} > 2k_{\text{b}}$. This expression is identical to the *point* input impedance of a beam of infinite length and unit width. This implies that the plate is locally reacting so that it can be physically replaced by a large number of narrow parallel-sided strips each having an impedance per unit width given by the above expression. The line impedance of a finite width plate attached to an infinite beam, for $k_{\text{p}} > 2k_{\text{b}}$, is shown to be given by

$$\tilde{Z}'_{\text{p}} = \frac{2m''_{\text{p}}\omega}{k_y}\left(\frac{1 - \tilde{\beta}_y}{1 + \tilde{\beta}_y} + \text{j}\right), \quad \tilde{\beta}_y = \text{e}^{-j\tilde{k}_y L_y}$$

where L_y = width of plate strip. An initial estimate of k_y is given by

$$\tilde{k}_y \approx k_{\text{p}}\sqrt{1 - s^2}\left(1 - \text{j}\frac{\eta_{\text{p}}}{4}\right), \quad s = \frac{k_{\text{b}}^{\infty}}{k_{\text{p}}}$$

This is then substituted into the above expression for $\tilde{Z}'_{\text{p}}$, which is then inserted into the dispersion relation

$$\tilde{D}_{\text{b}}k^4 = m'_{\text{b}}\omega^2 - \text{j}\omega Z$$

where $\tilde{D}_{\text{b}}$ = beam stiffness and m'_{b} = mass per unit length of the beam. The solution of this equation yields new beam wavenumbers. The process is repeated iteratively until the value of k_y converges. Having established a stable value of k_y it is now possible to obtain the transfer mobility Y_{bp} from the beam to the plate. This is

$$Y_{\text{bp}} = \frac{k_y}{m'_{\text{p}}\omega}\left(\frac{-\text{j}2\sqrt{\alpha_y}}{1 + \alpha_y}\right)$$

where $\alpha_y = \text{e}^{-\text{j}2k_y L_{\text{b}}}$. Grice then applies this concept to a box structure constructed from thin, flat plates, i.e. a much simplified car body model. Here, the load-carrying part (in this case, excluding the acoustics) is assumed to carry energy round the structure as

d000000199 13-12-06 16:24:58 Rev 14.05
The Charlesworth Group, Wakefield 01924 204830

in-plane rather than flexural motion. This energy is then converted into flexural motion at the panels that are likely to radiate sound into the cabin.

The technique was originally pioneered by Pinnington and Fig. 18 shows the box model set-up taken from one of his publications [**114**].

So far, verification has only been carried out on simple laboratory rigs. The main advantage of this method is that the models are very simple and a minimum of structural detail is required. Thus, it might be possible to obtain a general idea of the noise characteristics of a new vehicle at a very early stage. Furthermore, the very simplicity of the model makes it easier to understand the overall vibrational energy transfer mechanisms. However, it is unlikely to be as accurate as the previously described FEM/BEM or SEA methods.

A very interesting recent development, pioneered by Hauer [**115**], is the use of FEM models to theoretically calculate the SEA coupling loss factors. The advantage of this technique over just using an FEM model is that only FEM models of the two connected SEA subsystems need to be employed in order to calculate their coupling loss factors. This represents a considerable saving of computational effort, considering the very large size of the FEM model of a complete car. The author shows that predictions of sound pressure levels in the passenger cabin of a car, using an SEA model constructed in this way, are generally within 3 dB of the corresponding measurements.

6.4 Ray tracing method

This is quite an old concept and is particularly attractive for predicting noise in buildings that have an internally complex geometry, e.g. concert halls or factories. At present it is mainly an acoustic technique and there is a large body of literature on the subject. A good background to the theory as applied to simple geometries is given in an old (1967) paper by Krokstad *et al.* [**116**]. Later (in 1982) Kruzins and Fricke [**117**] showed how these concepts could be applied statistically to buildings of complex geometry. In the same year Tain-Fu and Er-Chang [**118**] demonstrated the relationship between the modal and ray representation of a sound field.

The basic concept as outlined by Krokstad *et al.* [**116**] is as follows. The calculation procedure uses a mathematical model of a hall, which is excited by a sound pulse emitted from a fixed point source. Energy is represented by rays equally distributed over the whole or over a selected part of the solid angle. The life history of each ray is calculated assuming geometrical reflection (with no losses) at all surfaces, until it strikes the audience area, where it is assumed to be totally absorbed. The points of impingement for all emitted rays and the time delay of the impingement relative to direct sound are calculated. As the rays are assumed to represent equal energy quanta, energy integration in space and time is performed simply by counting strikes. The number of

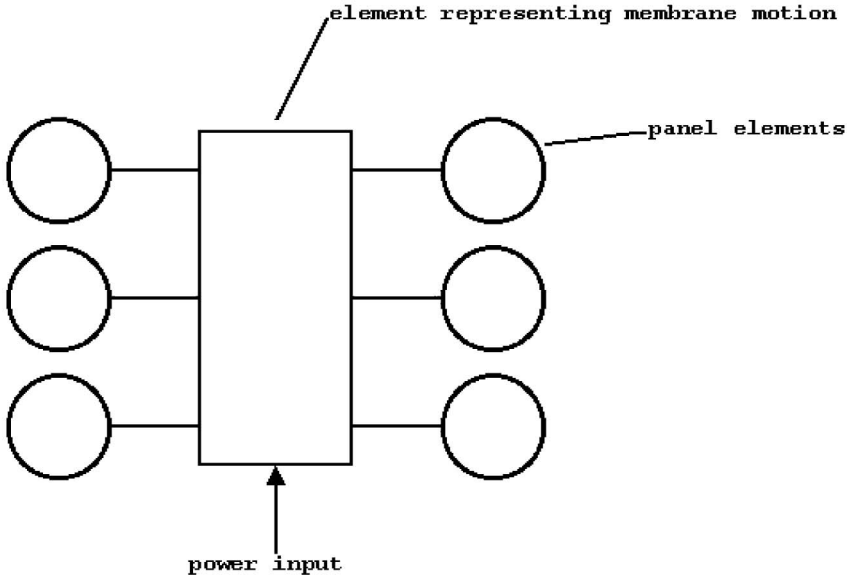

Fig. 18 Schematic diagram of the box model. (This material has been reproduced from *Autotech '93, Recent Advances in NVH Technology.* Application of SEA and power flow techniques to automotive structures, Figure 8, by R. J. Pinnington by permission of the Council of the Institution of Mechanical Engineers)

strikes into a control volume within a specified time frame is proportional to the sound intensity at that point in space and time. Details of the geometrical calculations used are given in the paper [**116**]. The recent vast increase in the available computer power has enabled much more complex building geometries, losses at reflections, and losses with distance to be included.

This theory, however, has only recently been applied to structural problems, in spite of the obvious potential advantages for the automotive application, i.e. power input can be at a specific point rather than generally into a subsystem and, similarly, the response can also be computed at a point. It is, of course, essential with this application to include losses with distance together with the energy lost, reflected, and transmitted at junctions. In a fairly recent paper, Chae and Ih [**119**] show how the classic ray tracing method (RTM) can be applied to an assembly of connected plates. If harmonic velocity is assumed, then the velocity at a point (x, y) will be

$$v = \hat{A} \exp[-\mathrm{j}(k_x x + k_y y)(1 - \mathrm{j}\eta/4)]$$

and the corresponding vibrational energy will be

$$\begin{aligned} e(x, y) &= T(x, y) + U(x, y) \\ &\approx \frac{1}{2} m'' |\hat{A}|^2 \exp\left[-\frac{\eta}{2}(k_x x + k_y y) \right] \\ &\equiv e_0 \exp\left[-\frac{\eta}{2}(k_x x + k_y y) \right] \end{aligned}$$

where $\hat{A}$ is the complex amplitude of the wave, $\mathrm{j} = \sqrt{-1}$, k_x and k_y are the wave numbers in the x and y directions respectively, $\eta =$ the structural loss factor, $T(x, y) =$ the kinetic energy, $U(x, y) =$ the potential energy, $m'' =$ the mass per unit area, and $e_0 =$ the energy density at the point $(0, 0)$.

The vibration intensity distribution due to this wave is given by

$$\boldsymbol{I}(x, y) \approx c_{\mathrm{g}} e(x, y) \boldsymbol{i}_\theta(x, y)$$

where $c_{\mathrm{g}} =$ the group velocity, $\boldsymbol{i}_\theta$ denotes the unit direction vector of $(k_x \boldsymbol{i}_x + k_y \boldsymbol{i}_y)/\sqrt{k_x^2 + k_y^2}$ or $(\cos\theta \cdot \boldsymbol{i}_x + \sin\theta \cdot \boldsymbol{i}_y)$, and $\boldsymbol{i}_x$, $\boldsymbol{i}_y$ are unit vectors in the x and y directions respectively. The authors assume that the vibrational energy travels along 'ray tubes'. When such a ray tube is incident upon the boundary between two coupled plates i and j, it can be considered equivalent to a plane wave, provided that its width is much less than the wavelength. With this assumption in mind, the authors then go on to show that the vibrational energy density of transmitted (e_j^{t}) and reflected (e_i^{r}) ray tubes at a coupling boundary is given by

$$e_j^{\mathrm{t}} = \tau_{12}(\phi_1)(c_{\mathrm{g}1}/c_{\mathrm{g}2})(\cos\phi_1/\cos\phi_2) e_i^i$$

$$e_i^{\mathrm{r}} = [1 - \tau_{12}(\phi)] e_i^i$$

where $\phi_1, \phi_2 =$ the incident and reflected ray tube angles respectively and $\tau_{12}(\phi) =$ the power transmission coefficient at the coupling boundary. By evaluating the energy at a number of receiver points, the vibrational energy distribution can be evaluated.

For simple structures the required parameters such as group velocities and power transmission coefficients are readily available, but they are much more difficult to determine for non-homogeneous structures such as car body shells. In addition, as the frequency is reduced, phase becomes increasingly important. Thus, this must primarily be considered as a high-frequency technique, as stated in reference [**17**]. However, Chae and Ih [**119**] state that the capabilities of this method might be extended to lower frequencies by band-averaging the results.

6.5 Band-averaged transfer function method

The concept of setting up a matrix of mobility vectors $(\mathbf{Y}_{ij})$ to describe the dynamic behaviour of a structure, i.e. $\boldsymbol{V} = \mathbf{Y}_{ij} \cdot \boldsymbol{F}$, where $\boldsymbol{V} =$ the velocity vector and $\boldsymbol{F} =$ the force vector, has been well established for many years. However, its use has been restricted to experimental applications, i.e. to find $\boldsymbol{V}$ when $\boldsymbol{F}$ is known or to find $\boldsymbol{F}$ when $\boldsymbol{V}$ is known, although it is notoriously difficult to accurately invert $\mathbf{Y}_{ij}$ to obtain $\boldsymbol{F}$ from known $\mathbf{Y}$'s, mainly because of the difficulty in obtaining accurate values for the rotational degrees of freedom.

However, Orefice [**120**] has introduced the concept of 'energetic mobility' $(|V_i|^2/P_j$, where $|V_i|^2 =$ mean square velocity at i and $P_j =$ input power at $j)$ that, provided certain conditions are met, has very significant advantages over the old method. Firstly, not all degrees of freedom now need to be taken into account and, secondly, the system is much more robust than before, so that inversion of the mobility matrix introduces far fewer errors. In addition to these factors, research into the method has revealed some slightly unexpected but very useful results. These are listed below:

1. *Energetic additivity.* If several input powers P_e are injected at points e on a structure with linear behaviour, they will produce a frequency-averaged

d000000199 13-12-06 16:24:58 Rev 14.05
The Charlesworth Group, Wakefield 01924 204830

squared velocity $\langle |V_m|^2 \rangle$ at any point m, viz.

$$\langle |V_m|^2 \rangle \approx \sum_{e=1}^{N_e} \mathbf{H}_{me} \cdot \mathbf{P}_e$$

where $\mathbf{H}_{me}$ = matrix of energetic mobilities.

2. *Energetic connectivity.* If two subsystems S^I and S^{II} are rigidly connected together at points c such that

$$\langle |\tilde{V}_c^I|^2 \rangle = \langle |\tilde{V}_c^{II}|^2 \rangle$$

and

$$\tilde{\mathbf{P}}_c^I = -\tilde{\mathbf{P}}_c^{II}$$

(where the tilde indicates quantities after coupling), then

$$\langle |\tilde{V}_m^I|^2 \rangle \approx \sum_{e=1}^{N_e^I} \mathbf{H}_{me}^I \cdot \tilde{\mathbf{P}}_e^I + \sum_{c=1}^{N_c} \mathbf{H}_{mc}^I \cdot \tilde{\mathbf{P}}_c^I$$

At present the technique is considered only as useful experimentally. However, the author does suggest a method of calculating **H** from established deterministic mobility formulae, which gives it a predictive capability. Because this method has some similarities with the SEA power balance equations it might be possible to incorporate Orefice's concept into the SEA theory. This would have the very significant advantage that SEA could then cater for power inputs and responses at specific points, rather than applying generally at the subsystem level.

7 CONCLUDING REMARKS

It can be reasonably assumed from the preceding discussion that the finite element (FEM) and/or boundary element (BEM) techniques described in section 6.1 are still the most suitable methods for predicting the low- and mid-frequency noise, as defined in this paper. This is primarily due to the fact that a passenger cabin has very few acoustic modes below 200 Hz. Thus, phase becomes very important so that frequency band averaged predictions, such as statistical energy analysis (SEA), described in section 6.2, would be expected to produce significant errors. However, due mainly to the variations in low-frequency damping, as discussed in section 5, it appears that actual variations of internal sound pressure levels in nominally identical cars are of similar magnitude to the errors induced by applying SEA at low frequencies. This means that in cases where only an average prediction is required, or where it is necessary to determine whether a proposed design change will have a detrimental or beneficial effect, SEA is still very useful, particularly because it is much quicker to create and run the models. The other methods described in sections 6 to 6.5 are still very much in their infancy and their application to the prediction of internal vehicle noise is still unproven. However, as they do potentially offer significant advantages over SEA, research into their development should be encouraged.

REFERENCES

1 **Jha, S. K.** and **Priede, T.** Origin of low frequency noise in motor cars. In Proceedings of the 14th FISITA Conference, 1972, Paper 1/8, p. 46

2 **Fung, K. K. H.** and **Zhu, J. J.** Investigation of acoustic leakage of vehicle dash pass-through components. SAE paper 971904, 1997.

3 **Tracey, B. H.** and **Huang, L.** Transmission loss for vehicle sound packages with foam layers. SAE paper 1999-01-1690, 1999.

4 **Yashiro, H., Suzuki, K., Kajio, Y., Hagiwara, I.,** and **Arai, A.** An application of structural–acoustic analysis to car body structure. SAE paper 850961, 1985.

5 **Winklhofer, E.** and **Thien, G. E.** A review of parameters affecting the noise and vibration in diesel powered passenger cars. SAE paper 850966, 1985.

6 **Kido, I., Nakamura, A., Hayashi, T.,** and **Asai, M.** Suspension vibration analysis for road noise using finite element model. SAE paper 1999-01-1788, 1999.

7 **Moeller, M. J.** and **Pan, J.** Statistical energy analysis for road noise simulation. SAE paper 971972, 1997.

8 **Lalor, N.** and **Bharj, T.** The application of SEA to the reduction of passenger car interior noise. In Proceedings of ISATA Conference on *Mechatronics*, Aachen, 1994, paper 94ME012.

9 **George, A. R.** Automobile aeroacoustics. In Proceedings of the 12th Aeroacoustics Conference, San Antonio, Texas, 1989, paper AIAA-89-1067.

10 **Strumolo, G. S.** The wind noise modeller. SAE paper 971921, 1997.

11 **Wood, L. A.** and **Joachim, C. A.** Variability of interior noise levels in passenger cars. In Proceedings of IMechE Conference, 1984, paper C136/84, p. 197.

12 **Kompella, M. S.** and **Bernhard, R. J.** Measurement of the statistical variation of structural–acoustic characteristics of automotive vehicles. SAE paper 931272, 1993.

13 **Gaardhagen, B.** and **Plunt, J.** Variation of vehicle NVH properties due to component eigenfrequency shifting – basic limits of predictability. SAE paper 951302, 1995.

14 **Ibrahim, R. A.** and **Pettit, C. L.** Uncertainties and dynamic problems of bolted joints and other fasteners. *JSV*, 2005, **279**(3–5), 857.

15 **Böhler, E., Wagner, G., Priebsch, H.-H., Bauer, M.,** and **Götzinger, B.** Berechnung akustischer verbesserungspotenziale von leichtbaukarosserien mittels FEM. *ATZ*, 10/2005, **107**, 880.

d000000199 13-12-06 16:24:58 Rev 14.05
The Charlesworth Group, Wakefield 01924 204830

16 **Kropp, A.** and **Ihlenburg, F.** Influence of local damping on the acoustic design of passenger car bodies. *Auto Technol.*, 4/2004.

17 **Sestieri, A., Del Vescoro, D.,** and **Lucibello, P.** Structural–acoustic coupling in complex shaped cavities. *JSV*, 1984, **96**(2), 219.

18 **Wilby, J. F.** Aircraft interior noise. *JSV*, 1996, **190**(3), 545.

19 **Rennison, D. C.** On the statistics of acoustic power flow through structures: tonal excitation. In Proceedings of Australian Acoustical Society International Conference on *Acoustics*, 1980, paper pD-9.5.

20 **Pope, L. D., Wilby, E. G., Willis, C. M.,** and **Mayes, W. H.** Aircraft interior noise models: sidewall trim, stiffened structures, and cabin acoustics with floor partition. *JSV*, July/August 1983, **89**(3), 371.

21 **Pope, L. D., Wilby, E. G.,** and **Wilby, J. F.** Propeller aircraft interior noise model: Pt I. Analytical model. *JSV*, 1987, **118**(3), 449.

22 **Pope, L. D., Willis, C. M.,** and **Mayes, W. H.** Pt II. Scale model and flight test comparisons. *JSV*, 1987, **118**(3), 469.

23 **Dunn, J. W., Olatunbosun, O. A.,** and **Mills, B.** Prediction of low frequency sound pressure distribution inside a vehicle passenger compartment from its structural dynamic response. *J. Sci. Environ. Engng*, 1980, **19**(3), 11.

24 **Koopmann, G. H.** and **Pollard, H. F.** A joint acceptance function for enclosed spaces. *JSV*, 1980, **73**(3), 429.

25 **Zienkiewicz, O. C.** *The finite element method*, 3rd edition (McGraw-Hill, Maidenhead).

26 **Petyt, M., Lea, J.,** and **Koopmann, G. H.** A finite element method for determining the acoustic modes of irregular shaped cavities. *JSV*, 1976, **45**(4), 495.

27 **Nefske, D. J., Wolf Jr, J. A.,** and **Howell, L. J.** Structural–acoustic finite element analysis of the passenger compartment: a review of current practice. *JSV*, January/February 1982, **80**(2), 247.

28 **Nefske, D. J.** and **Sung, S. H.** Vehicle interior acoustic design using finite element methods. *Int. J. Veh. Des.*, 1985, **6**(1), 24.

29 **Sung, S. H.** and **Nefske, D. J.** Component mode synthesis of a vehicle structural–acoustic system model. *Am. Inst. Aeronaut. Astronaut. J.*, 1986, **24**(6), 1021.

30 **Yashiro, H., Suzuki, K., Kajio, Y., Hagiwara, I.,** and **Arai, A.** An application of structural–acoustic analysis to car body structure. SAE paper 850961, 1985.

31 **Desmet, W., Sas, P.,** and **Vandepitte, D.** Performance of a wave based prediction technique for three-dimensional coupled vibro-acoustic analysis. In Proceedings of *EuroNoise 98*, Vol. 3, 1998, p. 913.

32 **Sas, P., Desmet, W., van Hal, V.,** and **Pluymers, B.** On the use of a wave based prediction technique for vehicle interior acoustics. In Proceedings of Styrian Noise, Vibration and Harshness Congress on *Integrated vehicle acoustics and comfort*, Graz, Austria, 2001.

33 **Hong, K. L.** and **Kim, J.** Analysis of free vibration of structural–acoustic coupled systems, Part 1: development and verification of the procedure. *JSV*, 1995, **188**(4), 561.

34 **Kopuz, S.** and **Lalor, N.** A note on structural–acoustic coupling phenomenon. ISVR Technical Memorandum 761, 1995.

35 **Cepkauskas, M. M.** and **Stevens, J.** A fluid–structure interaction via boundary operator method. *JSV*, September/October 1983, **90**(2), 229.

36 **Craggs, A.** Isochronous oscillators and their importance in low-frequency sound transmission in passenger vehicles. *JSV*, 1990, **142**(2), 360, Letter to editor.

37 **Morrey, D.** and **Whear, F. R.** An investigation of structural–acoustic interaction in the interior cavity of vehicle structures. In Proceedings of *Autotech 95*, 1995, paper C498/6/018.

38 **Jayachandran, V., Hirsch, S. M.,** and **Sun, J. Q.** On the numerical modelling of interior sound fields by the modal function expansion approach. *JSV*, 1998, **210**(2), 243.

39 **Crighton, D. G.** Rayleigh Medal Lecture: fluid loading – the interaction between sound and vibration. *JSV*, 1989, **133**(1), 1.

40 **Langley, R. S.** Dynamic stiffness boundary element method for the prediction of interior noise levels. *JSV*, 1993, **163**(2), 207.

41 **Luo, J.** and **Gea, H. C.** Modal sensitivity analysis of coupled acoustic–structural systems. *Trans. ASME*, 1997, **119**(4), 545.

42 **Sandberg, G.** and **Görensson, P.** A symmetric finite element formulation for acoustic fluid–structure interaction analysis. *JSV*, 1988, **123**(3), 507.

43 **Turner, W. B.** and **Turgay, F. M.** Development of coupled structure–acoustic FE models for vehicle refinement. In Proceedings of IMechE Conference on *Vehicle noise and vibration*, London, 1998, paper C521/026/98, p.229.

44 **Campbell, B., Abrishaman, M.,** and **Stokes, W.** Structural–acoustic analysis for the prediction of vehicle body acoustic sensitivities. SAE paper 931327, 1993.

45 **Tinti, F.** and **Scaffidi, C.** Improvement of interior acoustics of a top-class car in the low frequency range using a hybrid numerical–experimental technique. In Proceedings of the International Conference on *Computational acoustics and environmental applications*, COMPAC, 1997.

46 **Craggs, A.** A finite element model for acoustically lined small rooms. *JSV*, 1986, **108**(2), 327.

47 **Hong, K. L.** and **Kim, J.** New analysis method for general acoustic–structural coupled systems. *JSV*, 1996, **192**(2), 465.

48 **Sung, S. H., Nefske, D. J., Le-The, H.,** and **Bonarens, F.** Development and experimental evaluation of a vehicle structural–acoustic trimmed-body model. SAE paper 991798, 1999.

49 **Stokes, W., Bretl, J., Crewe, A., Park, W. S., Lee, J. Y.,** and **Lee, M. S.** Computer simulation of in-vehicle boom noise. SAE paper 971914, 1997.

50 Qian, Y. and **VanBuskirk, J.** Acoustic modeling and optimization of seat for boom noise. SAE paper 971950, 1997.

51 Kopuz, S. and **Lalor, L.** Analysis of interior acoustic fields using the finite element method and the boundary element method. *Appl. Acoust.*, 1995, **45**, 193.

52 Bennighof, J. K., Kaplan, M. F., Muller, M. B., and **Kim, M.** Meeting the NVH computational challenge: automated multi-level substructuring. In Proceedings of the 18th International Modal Analysis Conference, San Antonio, Texas, 2000.

53 Kropp, A. and **Heiserer, D.** Efficient broadband vibro-acoustic analysis of passenger car bodies using an FE-based component mode synthesis approach. *J. Comput. Acoust.*, 2003, **11**, 139–157.

54 Stryczek, R., Kropp, A., Wegner, S., and **Ihlenburg, F.** Vibro-acoustic computations in the mid-frequency range: efficiency, evaluation, and validation. In Proceedings of ISMA 2004, Leuven, Belgium, 2004, p. 1603.

55 Zhang, G., Castanier, M. P., Pierre, C., and **Mourelatos, Z. P.** Vibration and power flow analysis of a vehicle structure using characteristic constraint modes. SAE paper 2003-01-1602, 2003.

56 Zhang, G. *Component-based and parametric reduced-order modeling methods for vibration analysis of complex structures*, PhD Thesis, Mechanical Engineering Department, University of Michigan, 2005.

57 Becker, A. A. *The boundary element method in engineering* (McGraw-Hill, Maidenhead).

58 Suzuki, S., Imai, M., and **Maruyama, S.** Boundary element method for vehicle noise problems. In Proceedings of the ASME Winter Meeting on *Vehicle noise*, Dallas, Texas, 1990, NCA-Vol. 9, p. 17.

59 Sestieri, A. Discretization procedures for the Green formulation of structural–acoustic problems. *JSV*, January/February 1985, **98**(2), 305, Letter to the editor.

60 Succi, P. S. The interior acoustic field of an automobile cabin. *J. Acoust. Soc. Am.*, 1987, **81**(6), 1688.

61 Coyette, J. P. and **McCulloch, C. F.** Modelling interior and exterior acoustics using finite element and boundary element methods. In *Autotech 89 Noise control*, 1989.

62 Hussain, K. A. Rapid simulation of structural–acoustic interaction. In *Autotech 93, Noise and the automobile*, 1993.

63 Marburg, S. Calculation and visualization of influence co-efficients and acoustic contributions in vehicle cabins using mode superposition techniques. In Proceedings of the Computational Mechanics World Conference on *BEM*, 1996, p. 13.

64 Katsuta, T., Matsuda, A., and **Hamada, S.** Acoustic analysis of truck cab. SAE paper 911075, 1991.

65 Cheng, C. Y. R. and **Seybert, A. F.** Recent applications of the boundary element method to problems in acoustics. SAE paper 870997, 1987.

66 Utsuno, H. and **Inoue, K.** Analysis of the sound field in an automobile cabin by using the boundary element method. SAE paper 891153, 1989.

67 Suzuki, S., Maruyama, S., and **Ido, H.** Boundary element analysis of cavity noise problems with complicated boundary conditions. *JSV*, 1989, **130**(1), 79.

68 Sorokin, S. V. Analysis of vibrations of a spatial acoustic system by the boundary integral equations method. *JSV*, 1995, **180**(4), 657.

69 Soenarko, B. and **Seybert, A. F.** Recent developments of the boundary element method to noise control problems in automotive engineering. In Proceedings of the 6th Pacific Korean SAE Conference on *Automobile engineering*, 1991, p. 1339.

70 Cousins, P. L. and **Goodman, S. L.** A boundary integral and finite element coupled formulation for the modes in a three-dimensional cavity with a flexible panel. In Proceedings of IoA, 1990, paper B.4.2.1.

71 Frenchek, N. M. and **Bernhard, R. J.** Analytical, numerical and experimental comparisons of structure-borne noise in a rectangular acoustic enclosure. In Proceedings of NC NCE, INCE, 1994, p. p495.

72 Slepyan, L. I. and **Sorokin, S. V.** Analysis of structural–acoustic coupling problems by a two-level boundary integral method; Part 1: a general formulation and test problems. *JSV*, 1995, **184**(2), 195.

73 Sorokin, S. V. Analysis of structural–acoustic coupling problems by a two-level boundary integral equations method; Part 2: vibrations of a cylindrical shell of finite length in an acoustic medium. *JSV*, 1995, **184**(2), 213.

74 Everstine, G. C. Finite element formulations of structural acoustics problems. *Computers and structures*, 1997, **65**(7), 307.

75 Chen, Z. S., Svobodnik, A. J., and **Hofstetter, G.** Galerkin-type BE–FE formulation for elasto-acoustic coupling. *Comput. Meth. in Appl. Mechanics and Engng*, 1998, **152**(1–2), 147.

76 Urushiyama, Y. and **Nomoto, S.** Analysis of booming noise in a passenger compartment using boundary element method. *J. Soc. Automot. Engrs*, 1990, **11**(3), 45.

77 Seybert, A. F., Hu, T., Herrin, D. W., and **Ballinger, R. S.** Interior noise prediction process for heavy equipment cabs. SAE paper 971955, 1997.

78 Hargreaves, J. A. The use of indirect coupled boundary element analysis in vehicle NVH refinement. In Proceedings of the IMechE Conference on *Vehicle noise and bibration*, 1998, paper C521/019/98, p. 213.

79 McCulloch, C. F. and **Coyette, J.-P.** Recent advances in numerical acoustic modelling. In Proceedings of the IMechE Conference on *Vehicle NVH and refinement*, 1994, paper C487/023/94.

80 Cheng, K. W. *An investigation of modelling techniques for interior structure-borne noise generation mechanism*, PhD Thesis, Birmingham University, 1994.

81 Desmet, W. *A wave based prediction technique for coupled vibro-acoustic analysis*, PhD Thesis 98D12, KU Leuven, Belgium, 1998.

82 **Pluymers, B., Desmet, W., Vandepitte, D.,** and **Sas, P.** Feasibility study of the wave based method for high-frequency steady-state acoustic analysis. In Proceedings of ISMA 2004, Leuven, Belgium, 2004, p. 1555.

83 **van Hal, B., Vanmaele, C., Desmet, W., Silar, P.,** and **Priebsch, H.-H.** Hybrid finite element-wave based method for steady-state acoustic analysis. In Proceedings of ISMA 2004, Leuven, Belgium, 2004, p. 1629.

84 **Lyon, R. H.** SEA, power flow and energy accountancy. SAE paper 951303, 1995.

85 **DeJong, R. G.** A study of vehicle interior noise using statistical energy analysis. SAE paper 850960, 1985.

86 **Keane, A. J.** and **Price, W. G.** Statistical energy analysis of strongly coupled systems. *JSV*, 1987, **117**(2), 363.

87 **Craik, R. J. M., Steel, J. A.,** and **Evans, D. I.** SEA of structure-borne sound transmission at low frequencies. *JSV*, 1990, **144**(1), 95.

88 **Plunt, J.** On the use and misuse of statistical energy analysis for vehicle noise control. SAE paper 931301, 1993.

88 **Fredö, C. R.** Indirect couplings in energy flow models: can they be used to improve vehicle NVH predictions? SAE paper 951306, 1995.

90 **Cimerman, B., Bremner, P., Qian, Y.,** and **Van Buskirk, J. A.** Incorporating layered acoustic trim materials in body structural–acoustic models. SAE paper 951307, 1995.

91 **Powell, R. E., Zhu, J.,** and **Manning, J. E.** SEA modeling and testing for airborne transmission through vehicle sound package. SAE paper 971973, 1997.

92 **Liu, W., Taoand, D.,** and **Kathawate, G.** Use of statistical energy analysis method to predict sound transmission loss of sound barrier assemblies. SAE paper 991707, 1999.

93 **Onsay, T.** and **Akanda, A.** Transmission of structure-borne tire/road noise in a mid-size car: statistical energy analysis (SEA). In NC NCE, INCE, 1998, p. 543.

94 **Dong, B., Green, M., Voutyras, M., Bremner, P.,** and **Kasper, P.** Road noise modelling using statistical energy analysis method. SAE paper 951327, 1995.

95 **Parrett, A. V., Hicks, J. K., Burton, T. E.,** and **Hermans, L.** Statistical energy analysis of airborne and structure-borne automobile interior noise. SAE paper 971970, 1997.

96 **Moore, J. A., Powell, R.,** and **Bharj, T.** Development of condensed SEA models of passenger vehicles. SAE paper 991699, 1999.

97 **Moeller, M. J., Pan, J.,** and **DeJong, R. G.** A novel approach to statistical energy analysis model validation. SAE paper 951328, 1995.

98 **Chen, H.-Y., O'Keefe, M.,** and **Bremner, P.** A comparison of test-based and analytic SEA models for vibro-acoustics of a light truck. SAE paper 951329, 1995.

99 **Wang, D., Goetchius, G. M.,** and **Onsay, T.** Validation of a SEA model for a minivan: use of ideal air- and structure-borne sources. SAE paper 1999-01-1697, 1999.

100 **Manning, J. E.** Validation of SEA models using measured modal power. SAE paper 991703, 1999.

101 **Hermans, L.** and **Iadevaia, M.** Guidelines on the use of experimental SEA for modelling and understanding road noise in cars. SAE paper 991704, 1999.

102 **Beissner, K.** Acoustic radiation pressure in the near field. *JSV*, March/April 1984, **93**(4), 537.

103 **Nolte, B.** and **Gaul, L.** Sound energy flow in the acoustic near field of a vibrating plate. *M. Sys. Sig. Proc.*, 1996, **10**(3), 351.

104 **Steel, J. A.** Prediction of structural vibration transmission through a motor vehicle using statistical energy analysis. *JSV*, 1996, **193**(3), 691.

105 **Moeller, M. J.** and **Powell, R. E.** Review of statistical energy analysis (SEA) applied to the automotive industry 1985 to 1997. NC NCE, INCE, 1998.

106 **Langley, R. S.** and **Brown, A. W. M.** Natural frequency statistics and response variance prediction. In Proceedings of the Second International Auto-SEA Users Conference, Michigan, 2002.

107 **Bitsie, F.** and **Bernhard, R.** Structure-borne noise prediction using an energy finite element method. SAE paper 972009, 1997.

108 **Gur, Y., Wagner, D. A.,** and **Morman, K. N.** Energy finite element analysis methods for mid-frequency NVH applications. SAE paper 1999-01-1801, 1999.

109 **Bonilha, M. W.** and **Fahy, F. J.** Measurements of vibration field correlation on a car body shell. *Appl. Acoust.*, 1994, **43**, 1.

110 **Bonilha, M. W.** *A hybrid deterministic–probabilistic model for vibroacoustic studies*, PhD Thesis, ISVR, Southampton University, 1996.

111 **Heidari, M. A.** and **Marshall, S. E.** Integrated FEM–SEA technique for predicting engine vibration noise in commercial airplanes. In Proceedings of NC NCE, Vol. 1, INCE, 1996, p. 151.

112 **Langley, R. S.** and **Bremner, P.** A hybrid method for the vibration analysis of complex structural–acoustic systems. *J. Acoust. Soc. Am.*, 1999, **105**(3).

113 **Grice, R. M.** *Vibration analysis of built-up structures by combining finite element analysis and analytical impedances*, PhD Thesis, ISVR, Southampton University, 1998.

114 **Pinnington, R. J.** Application of SEA and power flow techniques to automotive structures. In *Autotech 93' Noise and the automobile*, 1993.

115 **Hauer, I.** *A predictive hybrid approach for SEA*, PhD Thesis, Technical University of Graz, Austria, 2004.

116 **Krokstad, A., Strom, S.,** and **Sørsdal, S.** Calculating the acoustical room response by the use of a ray tracing technique. *JSV*, 1968, **8**(1), 118.

117 **Kruzins, E.** and **Fricke, F.** The prediction of sound fields in non-diffuse spaces by a 'random walk' approach. *JSV*, March/April 1982, **81**(4), 549.

118 **Gao Tain-Fu** and **Shang Er-Chang** The transformation between the mode representation and the generalised ray representation of a sound field. *JSV*, January/February 1982, **80**(1), 105.

119 **Chae, K.-S.** and **Ih, J.-G.** Prediction of vibrational energy distribution in two-dimensional structures at high frequency bands by using the ray tracing method. Paper presented to *J. Sound and Vibr.*, 2000.

120 **Orefice, G.** *Description par mobilites energetiques des echanges vibratoires dans les systemes couples*, PhD Thesis, INSA, Lyon, France, 1997.